

**COMPACTED BENTONITE-CRUSHED SALT
MIXTURES AS SEALANTS IN MINE OPENINGS**



Usachon Niewphueng

A Thesis Submitted in Partial Fulfillment of the Requirements for the

Degree of Master of Engineering in Geotechnology

Suranaree University of Technology

Academic Year 2016

การบดอัดเบนทอไนต์ผสมเกลือหินบด
เพื่อเป็นวัสดุถมกลับในช่องเหมือง



นางสาวอุษาชล เหนี่ยวผึ้ง

วิทยานิพนธ์นี้เป็นส่วนหนึ่งของการศึกษาตามหลักสูตรปริญญาวิศวกรรมศาสตรมหาบัณฑิต
สาขาวิชาเทคโนโลยีธรณี
มหาวิทยาลัยเทคโนโลยีสุรนารี
ปีการศึกษา 2559

COMPACTED BENTONITE-CRUSHED SALT MIXTURES

AS SEALANTS IN MINE OPENINGS

Suranaree University of Technology has approved this thesis submitted in partial fulfillment of the requirements for a Master's Degree.

Thesis Examining Committee



(Asst. Prof. Dr. Decho Phueakphum)

Chairperson



(Dr. Prachya Tepnarong)

Member (Thesis Advisor)



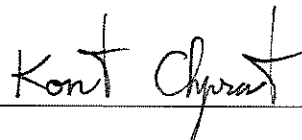
(Prof. Dr. Kittitep Fuenkajorn)

Member



(Prof. Dr. Sukit Limpijumnong)

Vice Rector for Academic Affairs
and Innovation



(Assoc. Prof. Ft. Lt. Dr. Kontorn Chamniprasart)

Dean of Institute of Engineering

อุษาชล เหนี่ยวผิง : การบดอัดเบนทอไนต์ผสมเกลือหินบดเพื่อเป็นวัสดุถมกลับในช่อง
เหมือง (COMPACTED BENTONITE-CRUSHED SALT MIXTURES AS SEALANTS
IN MINE OPENINGS) อาจารย์ที่ปรึกษา : อาจารย์ ดร.ปรัชญา เทพนรงค์, 83 หน้า.

วัตถุประสงค์ของการศึกษานี้คือ เพื่อศึกษาศักยภาพเชิงกลศาสตร์ของส่วนผสมด้วยวิธีการ
บดอัดระหว่างเบนทอไนต์และเกลือหินบดในน้ำเกลืออิ่มตัวสำหรับใช้เป็นวัสดุอุด เกลือหินบดมี
ขนาดคละกันระหว่าง 0.075 ถึง 2.35 มิลลิเมตร อัตราส่วนของเบนทอไนต์และเกลือหินบดผันแปร
จาก 10:90 ถึง 100:0 โดยน้ำหนัก การทดสอบกำลังรับแรงเฉือน โดยตรง ได้ถูกดำเนินการเพื่อหา
ความต้านทานแรงเฉือนของส่วนผสม และการทดสอบการบวมตัวได้ดำเนินการเพื่อหาอัตราการ
บวมตัวหลังการบดอัด ผลการทดสอบระบุว่ากำลังรับแรงกดในแกนเดียว สัมประสิทธิ์ความยืดหยุ่น
อัตราส่วนปัวซงของ มุมเสียดทาน และความเค้นยึดติดมีค่าเพิ่มขึ้นเมื่อปริมาณของเบนทอไนต์ลดลง
นอกจากนี้ความสามารถในการบวมตัวมีค่าเพิ่มขึ้นเมื่อปริมาณของเบนทอไนต์เพิ่มขึ้น แบบจำลอง
ทางคอมพิวเตอร์ได้ถูกใช้ในการหาประสิทธิภาพของวัสดุถมกลับในเหมืองเกลือเพื่อลดการทรุดตัว
ของผิวดินหลังการขุดเจาะช่องเหมือง การทรุดตัวและการเปลี่ยนแปลงรูปร่างของช่องเหมือง
เพิ่มขึ้นตามความลึกและความสูงของช่องเหมือง และลดลงเมื่ออัตราส่วนเบนทอไนต์และเกลือหิน
บดลดลง การเพิ่มขึ้นของอัตราส่วนเบนทอไนต์และเกลือหินบดอาจเหมาะสมสำหรับใช้เพื่อลดการ
หมุนเวียนของน้ำบาดาล อย่างไรก็ตามในบริเวณที่จำเป็นต้องใช้วัสดุถมกลับที่มีความแข็งแรงการ
ลดลงของอัตราส่วนเบนทอไนต์และเกลือหินบดอาจมีความเหมาะสมมากกว่า

สาขาวิชา เทคโนโลยีธรณี
ปีการศึกษา 2559

ลายมือชื่อนักศึกษา อุษาชล เหนี่ยวผิง
ลายมือชื่ออาจารย์ที่ปรึกษา Dr. P. Tepran

USACHON NIEWPHUENG : COMPACTED BENTONITE-CRUSHED
SALT MIXTURES AS SEALANTS IN MINE OPENINGS.

THESIS ADVISOR : PRACHYA TEPNARONG, Ph.D., 83 PP.

COMPACTION /SHEAR STRENGTH/CRUSHED SALT/BENTONITE

The objective of this study is to determine the mechanical performance of compacted bentonite-to-crushed salt mixtures with saturated brine for use as the sealing materials. The grain sizes of the crushed salt range from 0.075 to 2.35 mm. The mixture have bentonite-to-crushed salt ratios ranging from 10:90 to 100:0. Direct shear tests are conducted to determine the shearing resistance of the mixtures. Swelling tests are performed to determine the swelling capacity after compaction. The results indicate that the lower bentonite content specimens has higher uniaxial strength, elastic modulus, Poisson's ratio, friction angle and cohesion. The swelling capacity increases with increasing bentonite content. The computer simulations are used to determine the effectiveness of backfill in salt mines to reduce surface subsidence after excavation. The subsidence and opening deformations increase with mining depth and opening height. The subsidence and opening deformations decrease with decreasing B:C ratios. The higher B:C ratio may be suitable for minimizing groundwater circulation. In the area where backfill strength is required, the lower B:C ratios may be more appropriate.

School of Geotechnology

Academic Year 2016

Student's Signature ชัชวาล เตพนารอง

Advisor's Signature P. Tepranong

ACKNOWLEDGMENTS

I wish to acknowledge the funding supported by Suranaree University of Technology (SUT).

I would like to express my sincere thanks to Dr. Prachya Tepnarong for his valuable guidance and efficient supervision. I appreciate his strong support, encouragement, suggestions and comments during the research period. My heartiness thanks to Prof. Dr. Kittitep Fuenkajorn and Asst. Prof. Dr. Decho Phueakphum for their constructive advice, valuable suggestions and comments on my research works as thesis committee members. Grateful thanks are given to all staffs of Geomechanics Research Unit, Institute of Engineering who supported my work.

Finally, I would like to thank beloved parents for their love, support and encouragement.

Usachon Niewphueng

มหาวิทยาลัยเทคโนโลยีสุรนารี

TABLE OF CONTENTS

	Page
ABSTRACT (THAI)	I
ABSTRACT (ENGLISH).....	II
ACKNOWLEDGEMENTS	III
TABLE OF CONTENTS.....	IV
LIST OF TABLES	VIII
LIST OF FIGURES	IX
SYMBOLS AND ABBREVIATIONS.....	XIV
CHAPTER	
I INTRODUCTION	1
1.1 Background and rationale.....	1
1.2 Research objectives.....	1
1.3 Research methodology.....	2
1.3.1 Literature review	2
1.3.2 Sample Preparation.....	2
1.3.3 Compaction Test	2
1.3.4 Direct Shear Test.....	4
1.3.5 Uniaxial Compression Test.....	4
1.3.6 Swelling Test	4
1.3.7 Wet-Dry Cycle Test	4

TABLE OF CONTENTS (Continued)

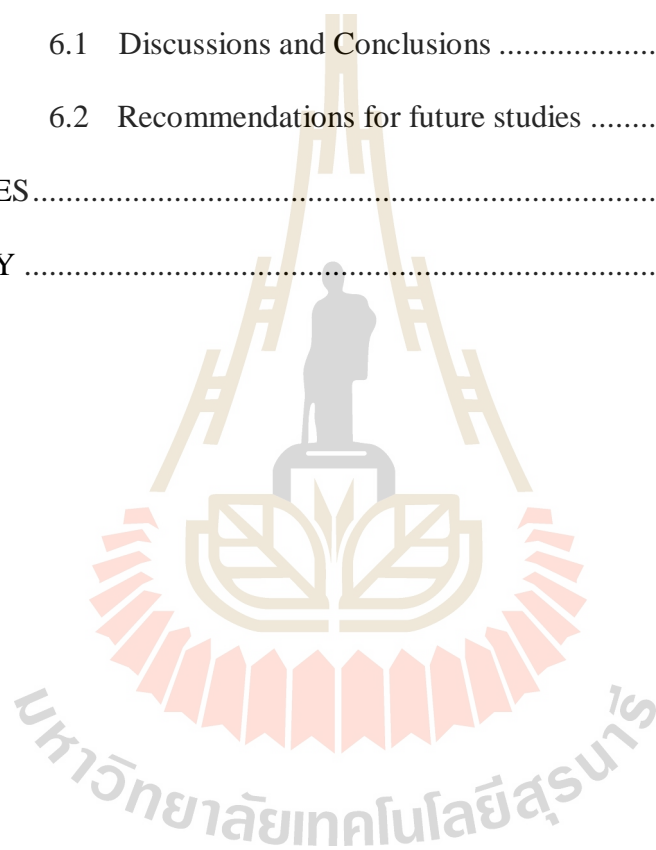
	Page
1.3.8 Swelling under Constant Load Tests	5
1.3.9 Result Analysis	5
1.3.10 Computer Simulations	5
1.3.11 Discussions, Conclusions and Thesis writing.....	5
1.4 Scope and limitations of the study	6
1.5 Thesis contents.....	7
II LITERATURE REVIEW	7
2.1 Introduction	7
2.2 Experimental researches on sealing/backfill materials	7
2.3 Direct Shear Test.....	13
2.4 Laboratory Test.....	15
2.5 Numerical simulations.....	19
III SAMPLE PREPARATIONS	21
3.1 Introduction	21
3.2 Sample preparation	21
3.2.1 Bentonite.....	21
3.2.1.1 Initial water content of air-dried bentonite	21
3.2.1.2 Specific gravity	22
3.2.1.3 Atterberg's limit	22
3.2.2 Crushed salt	23

TABLE OF CONTENTS (Continued)

	Page
3.2.3 Saturated brine	24
3.2.4 Bentonite and crushed salt mixtures	24
IV TEST METHOD AND RESULTS	29
4.1 Introduction	29
4.2 Test Equipment for Compaction and Direct Shear Tests	29
4.3 Compaction Test Method and Results	30
4.4 Direct Shear Test Method and Results	33
4.5 Swelling Test Method and Results	38
4.5.1 Wet-Dry Cycles Test Method and Results	38
4.5.2 Swelling under Constant Loads Test Method and Results	40
4.6 Uniaxial Compressive Strength Tests Method and Results	43
V COMPUTER SIMULATIONS	46
5.1 Introduction	46
5.2 Input parameters.....	46
5.3 Simulation results.....	47
5.3.1 Duration before backfill	47
5.3.2 Opening height.....	47
5.3.3 Overburden thicknesses.....	48
5.4 Discussions	50

TABLE OF CONTENTS (Continued)

	Page
VI DISCUSSIONS, CONCLUSIONS RECOMMENDATIONS FOR FUTURE STUDIES.....	75
6.1 Discussions and Conclusions	75
6.2 Recommendations for future studies	76
REFERENCES.....	77
BIOGRAPHY	83



LIST OF TABLES

Table	Page
2.1 Alternative Proctor Test Methods (Reddy, 2005).....	18
3.1 Engineering basic properties of bentonite.....	23
3.2 Typical chemical compositions of bentonite.and crushed salt samples.....	27
3.3 Chemical compositions of crushed salt obtained by XRF analysis (Khamrat, 2016).....	28
4.1 Compaction test results.....	32
4.2 Direct shear test results.....	37
4.3 Uniaxial compressive strength results.....	44
5.1 Mechanical properties of clastic rock and rock salt for FLAC 4.0 simulations (Crosby 2007, Sriapai et al, 2012).....	49
5.2 Time-dependent properties of rock salt for FLAC 4.0 simulations (Samsri et al., 2010).....	49
5.3 Compacted material properties for FLAC 4.0 simulations.....	50
5.4 Results of surface subsidence.....	72
5.5 Results of roof deformation.....	72
5.6 Results of floor heap.....	73
5.7 Results of pillar expansion.....	73
5.8 Results of pillar yield.....	74

LIST OF FIGURES

Figure	Page
1.1 Research methodology.....	3
2.1 Direct shear box (Das, 2010).....	13
2.2 Nature of residual shear strength and peak shear strength (Das, 2010).....	14
2.3 Mohr-Coulomb criterion as a function of shear strengths and normal stresses (Das, 2010).....	14
2.4 Proctor compaction test result (Proctor, 1933).....	19
3.1 Bentonite obtained from Thai Nippon Chemical Industry Co., LTD, Thailand.....	25
3.2 Crushed salt from a hammer mill machine.....	25
3.3 Grain size distribution of crushed salt.....	26
3.4 Bentonite and crushed salt are mixes with saturated brine.....	26
4.1 Three-ring compaction mold (a) and direct shear test frame developed for use with the three-ring mold (b) (Sonsakul and Fuenkajorn, 2013).....	30
4.2 Relationship between dry density and brine content as function of bentonite content.....	32
4.3 Three ring mold in the direct shear frame.....	34
4.4 Shear stresses as a function of shear displacement.....	35

LIST OF FIGURES (Continued)

Figure	Page
4.5 Shear strength as a function of normal stress.....	36
4.6 Friction angle as a function of bentonite content.....	36
4.7 Cohesion as a function of bentonite content.....	37
4.8 Swelling test in three-ring compaction mold.....	39
4.9 Swelling ratio as a function of time.....	39
4.10 Swelling ratio as a function of time for 3 cycles.....	41
4.11 Swelling ratio of bentonite-crushed salt mixtures as a function of time under load 4.5 kg (a), 9.0 kg (b) and 13.5 kg (c).....	42
4.12 Swelling ratio of bentonite-crushed salt mixtures as a function of static load.....	43
4.13 Post-tested bentonite-crushed salt mixture specimens after uniaxial compressive strength testing.....	44
4.14 Uniaxial stress-strain curves of specimens.....	45
5.1 Stratigraphy of borehole no. K-089 at Ban Hhao, Muang district, Udon Thani province (Suwanich, 1986).....	48
5.2 Mesh and boundary conditions used in this study.....	51
5.3 Surface subsidence as a function of time with different B:C ratios where overburden thicknesses 200 m, duration before backfill 6, 12 and 24 months, and opening height 6 m.....	52

LIST OF FIGURES (Continued)

Figure		Page
5.4	Roof deformation as a function of time with different B:C ratios where overburden thicknesses 200 m, duration before backfill 6, 12 and 24 months, and opening height 6 m.....	53
5.5	Floor heap as a function of time with different B:C ratios where overburden thicknesses 200 m, duration before backfill 6, 12 and 24 months, and opening height 6 m.....	54
5.6	Pillar expansion as a function of time with different B:C ratios where overburden thicknesses 200 m, duration before backfill 6, 12 and 24 months, and opening height 6 m.....	55
5.7	Pillar yield as a function of time with different B:C ratios where overburden thicknesses 200 m, duration before backfill 6, 12 and 24 months, and opening height 6 m.....	56
5.8	Finite difference mesh for opening height 6, 8 and 10 m, overburden thickness 300 m and rock salt 30 m.....	57
5.9	Surface subsidence as a function of time for different B:C ratios where opening height 6, 8 and 10 m, overburden thicknesses 300 m and duration before backfill 24 months.....	58
5.10	Roof deformation as a function of time for different B:C ratios where opening height 6, 8 and 10 m, overburden thicknesses 300 m and duration before backfill 24 months.....	59

LIST OF FIGURES (Continued)

Figure	Page
5.11 Floor heap as a function of time for different B:C ratios where opening height 6, 8 and 10 m, overburden thicknesses 300 m and duration before backfill 24 months.....	60
5.12 Pillar expansion as a function of time for different B:C ratios where opening height 6, 8 and 10 m, overburden thicknesses 300 m and duration before backfill 24 months.....	61
5.13 Pillar yield as a function of time for different B:C ratios where opening height 6, 8 and 10 m, overburden thicknesses 300 m and duration before backfill 24 months.....	62
5.14 Finite difference mesh for overburden thickness 200, 250 and 300 m, rock salt 30 m and opening height 6 m.....	63
5.15 Surface subsidence as a function of time for different B:C ratios where overburden thicknesses 200, 250 and 300 m, duration before backfill 24 months and opening height 6 m.....	64
5.16 Roof deformation as a function of time for different B:C ratios where overburden thicknesses 200, 250 and 300 m, duration before backfill 24 months and opening height 6 m.....	65
5.17 Floor heap as a function of time for different B:C ratios where overburden thicknesses 200, 250 and 300 m, duration before backfill 24 months and opening height 6 m.....	66

LIST OF FIGURES (Continued)

Figure		Page
5.18	Pillar expansion as a function of time for different B:C ratios where overburden thicknesses 200, 250 and 300 m, duration before backfill 24 months and opening height 6 m.....	67
5.19	Pillar yield as a function of time for different B:C ratios where overburden thicknesses 200, 250 and 300 m, duration before backfill 24 months and opening height 6 m.....	68
5.20	Subsidence reduction as a function of bentonite content.....	69
5.21	Roof deformation reduction as a function of bentonite content.....	69
5.22	Floor heap reduction as a function of bentonite content.....	70
5.23	Pillar expansion reduction as a function of bentonite content.....	70
5.24	Pillar yield reduction as a function of bentonite content.....	71

SYMBOLS AND ABBREVIATIONS

ρ	=	Density
c	=	Cohesion
ϕ	=	Friction angle
σ_n	=	Normal stress
τ	=	Shear stress
e	=	Void ratio
ν	=	Poisson's ratio
σ_c	=	Uniaxial compressive strengths
H	=	initial height
ΔH	=	Height Different
W_B	=	Brine content

CHAPTER I

INTRODUCTION

1.1 Background of problems and significance of the study

Mine openings require sealing to prevent brine leak around the openings in of salt and potash mines. The important properties of sealing materials are hydraulic conductivity, swelling ability and mechanical properties. The material should be easy to handle and compatibility with host rock formation (Fuenkajorn and Daemen, 1996; Mahir, 2007). Bentonite has become widely as a sealing material because of its ability to perform these functions. Crushed salt is an attractive candidate because it is readily available from the mining operations and compatible with the host rock.

The compacted bentonite based other materials (e.g. sand, crushed rocks) have been proposed as sealing in the disposal of hazardous wastes in salt mines, abandoned open pits or abandoned underground mined openings can be demonstrated to be practical and acceptable because the properties of mixtures better than those of the pure bentonite whereas the price is lower (Ouyang and Daeman, 1992).

1.2 Research objectives

The objectives of this study are determine the mechanical performance of compacted bentonite and crushed salt mixtures with saturated brine under ambient temperatures. The efforts include compaction test, direct shear test, and swelling test. FLAC 4.0 code is used to simulate the opening deformability and surface subsidence before and after backfilling. The findings can be useful to design the sealing material for opening in salt mines.

1.3 Research methodology

The research methodology shown in Figure 1.1 comprises 9 steps; including literature review, sample preparation, compaction test, direct shear test under various normal loads, uniaxial compression test, swelling test, wet-dry cycles test, swelling under constant loading test, results analysis, computer simulation, discussions and conclusions and thesis writing.

1.3.1 Literature Review

Literature reviews are carried out to study the experimental researches on the compacted bentonite based materials, direct shear test and swelling tests. The sources of information are from textbooks, journals, technical reports and conference papers. A summary of the literature review will be given in the thesis.

1.3.2 Sample Preparation

Bentonite and crushed salt are used as sealing materials in this study. Bentonite has been obtained from Thai Nippon Chemical Industry Co., LTD, Thailand. Crushed salt is from the Middle Members of the Maha Sarakham Formation, northeastern Thailand. Saturated brine is prepared by mixing pure salt with distilled water in the plastic tank.

1.3.3 Compaction Test

Compaction test performed according to the ASTM standard determine the optimum brine content and maximum dry densities of samples. The standard mold and the three rings mold (Sonsakul and Fuenkajorn, 2013) are used in this study. Results of compacted pure bentonite with saturated brine are comparing with the standard and three rings mold.

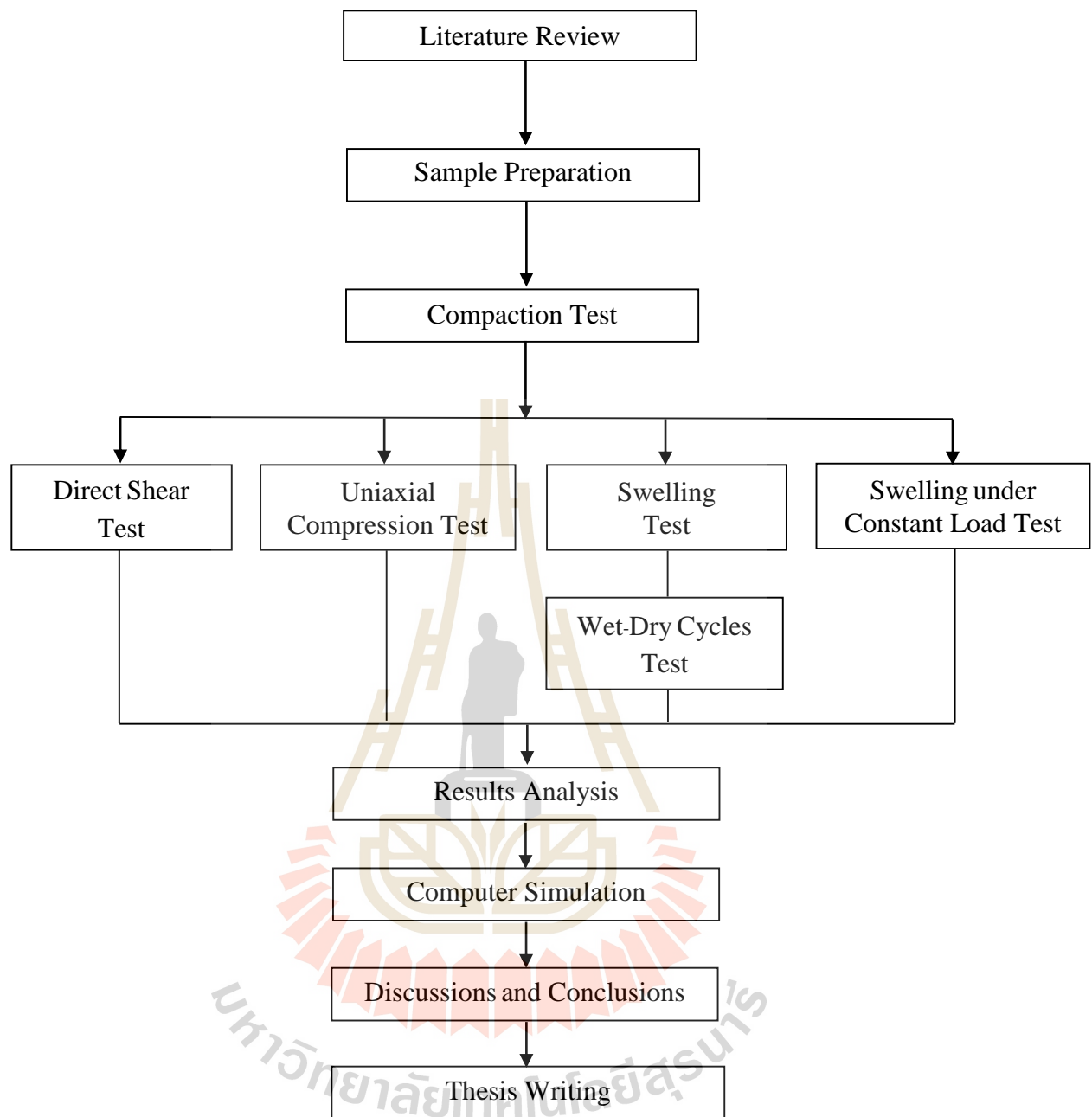


Figure 1.1 Research methodology.

The bentonite (B) and crushed salt (C) mixture ratios of 100:0, 90:10, 80:20, 70:30, 60:40, 50:50, 40:60, 30:70, 20:80 and 10:90 by weight are mixed with saturated brine at 0 to 40% by weight.

1.3.4 Direct Shear Test

The direct shear tests are performed to determine shear strength of compacted bentonite-crushed salt mixtures. The normal force is applied by the vertical hydraulic load cell ranging from 0.1, 0.3, 0.5 and 0.6 MPa.

1.3.5 Uniaxial Compression Test

The compressive strength, elastic properties and Poisson's ratio of the compacted B:C ratios 40:60, 60:40 and 80:20 are determined by axially loading the mixtures (after removing from the three ring mold). The results are used as parameters in FLAC simulations.

1.3.6 Swelling Test

The objective of swelling tests is to determine the swelling ability as a function of times of the compacted bentonite - crushed salt mixtures. Each sample is compacted in the three rings mold for 27 times, in six layers. The brine are added on specimen all the times till 30 days. Swelling is recorded every 10 minutes.

1.3.7 Wet-Dry Cycle Test

The wet-dry cycle tests are performed to investigate the effect of wet-dry conditions on samples. The specimen was wetted for 10 days. After 10 days. The specimens are dried by the oven at 70 °c for 15 days. Such cycles of wetting and drying are repeated up to 3 cycles.

1.3.8 Swelling under Constant Load Tests

The samples are swelled under loads of 4.5, 9.0 to 13.5 kg, to determine the swelling ratio of compacted bentonite - crushed salt mixtures.

1.3.9 Result Analysis

The research results are analyzed to optimize the bentonite - crushed salt mixtures in terms of the mechanical and swelling properties. The results of the analysis are used in the comparison with other researches.

1.3.10 Computer Simulations

The computer simulations is performed to determine the effectiveness of backfill in salt and potash mines after the excavation completed. The finite difference analyses are performed using FLAC 4.0 (Itasca, 1992) to assess the time-dependent surface subsidence and the deformation of rooms and pillars.

1.3.11 Discussions, Conclusions and Thesis writing

Discussions of the results are described to determine the reliability and accuracy of the measurements. Performance of the sealing material is discussed based on the test results. Similarities and discrepancies of the sealing material in terms of the mechanical properties are discussed to apply in the fields. All research activities, methods, and results are documented and complied in the thesis. The research or findings will be published in the conference proceedings or journals

1.4 Scope and limitations of the study

The scope and limitation of the research include as follows.

1. Bentonite in this study is from Thai Nippon Chemical Industry Co., LTD, Thailand.
2. Crushed salt specimens are from the Lower Members of the Maha Sarakham formation. The crushed salt has grain sizes ranging from 0.075 to 2.36 mm.
3. Compaction test is performed with bentonite-crushed salt mixtures consisting of different crushed salt content of 10, 20, 30, 40, 50, 60, 70, 80 and 90 percentages.
4. Direct shear testing uses three-ring direct shear device under normal stresses varies from 0.1, 0.3, 0.5 and 0.6 MPa.
5. Uniaxial compression tests are performed on the specimens after removing from the three rings mold.
6. Swelling tests follow the ASTM standard practice.
7. Wet-dry cycles test is 10 days. After 10 days, the specimens are dried by the oven at 70 °c for 15 days. The specimen are repeated up to 3 cycles.
8. Specimens are swelled under constants load varying from 4.5, 9.0 to 13.5 kg.
9. All tests are conducted under ambient temperature.
10. No field testing are performed.

1.5 Thesis contents

Chapter one describes the background of problems and significance of the study. The research objectives, methodology, scope and limitations are identified. Chapter two summarizes the results of the literature review. Chapter three describes the sample and mixture preparations. Chapter four describes the results from the laboratory experiments. Chapter five discusses and concludes the research results, and provides recommendations for future research studies.



CHAPTER II

LITERATURE REVIEW

2.1 Introduction

This chapter summarizes the results of literature review carried out to improve an understanding of the, which include recent research results and utilization of the bentonite, crushed salt or bentonite and crushed rock for sealing material, compaction test and direct shear test.

2.2 Experimental researches on sealing/backfill materials

Fuenkajorn and Daemen (1987) study the mechanical relationship between cement, bentonite and surrounding rock. The study deals with the mechanical interaction between multiple plugs and surrounding rock and identification of potential failure. Two conceptual plug designs are studied. Pipe tests have been performed to determine the swelling pressures of 60 mm diameter bentonite plugs and of 64 mm diameter cement plugs. The axial and radial swelling pressures of a bentonite plug specimen are 7.5 and 2.6 MPa after adsorbing water for 5 days. The maximum radial expansive stresses of the cement plugs cured for 25 days are 4.7 and 2.7 MPa for system 1 and system 3 cements. Results from the experiment indicate that in order to obtain sufficient mechanical stability of bentonite seal, the sealing should be done below groundwater level. If cement material is used to seal in hard rock, the mechanical stability will be higher than sealing in soft rock.

Case and Kelsall (1987) study the potential of crushed for required sealing access shafts and drifts for long periods. Crushed salt backfill is being investigated as a potential backfill and seal material through laboratory testing to determine how fundamental properties such as permeability, porosity and creep rate are reduced by pressure and time through consolidation. The test program reported in this paper consisted of four consolidation tests using crushed salt obtained from the Waste Isolation Pilot Plant and the Avery Island Mine. Tests with one- or two-month durations were conducted on samples with maximum particle sizes of 1, 10, and 20 mm, with initial porosities ranging from 26 to 36%, moisture contents of zero and 2%, and initial permeability from 10^3 to 10^5 m². The tests were performed at ambient temperature and confining pressures ranging from 0.34 MPa to 17 MPa. The most significant observation from the tests was the influence of moisture on changes in permeability, porosity and volumetric creep strain rate. The final permeability and porosity of one moist sample were reduced after one month to about 10^{-5} m² and 5%, respectively, compared to about 10^{-2} m² and 14 to 19% for the dry samples. In addition, the consolidation rate for the moist sample was more rapid at comparable porosities. In all of the tests, the volumetric creep strain rate ranged from 10^{-8} to 10^{-6} /sec, and did not achieve steady state values after 1 to 2 months of load application.

Butcher (1991) concluded that a 70% by weight salt and 30 % by weight bentonite mixture is preferable to pure crushed salt as backfill for disposal rooms in the Waste Isolation Pilot Plant. The performance of two backfill materials is examined with regard to various selection criteria related to compliance with transuranic radioactive waste standard 40 CFR 191, Subpart B, such as the need for low liquid permeability after closure, chemical stability, strength, ease of emplacement, and

sorption potential for brine and radionuclides. Both salt and salt/bentonite are expected to consolidate to a final state of permeability $\leq 10^{-18} \text{ m}^2$, which is adequate for satisfying government regulations for nuclear repositories. The real advantage of the salt/bentonite backfill depends, therefore, on bentonite's potential for absorbing brine and radionuclides. Estimates of the impact of these properties on backfill performance are presented.

Ouyang and Daemen (1992) study the sealing performance of American Colloid C/S granular bentonite and crushed Apache Leap tuff. Bentonite weight percent and crushed tuff gradation are the major variables studied. The sealing performance assessments include high injection pressure flow tests, polyaxial flow tests, high temperature flow tests, and piping tests. The results indicate that a composition would have at least 25% bentonite by weight mixed with well-graded crushed rock. Hydraulic properties of the mixture plugs may be highly anisotropic if significant particle segregation occurs during sample installation and compaction. Temperature has no significant effect on the sealing performance within the test range from room temperature to 60°C. Piping damage to the sealing performance is small if the maximum hydraulic gradient does not exceed 120 and 280 for samples with a bentonite content of 25 and 35%, respectively.

Hansen (1997) study the dynamic compacted crushed salt. The material has the moisture contents of 1.6 % by weight. The test procedures included shear consolidation, constant strain rate and permeability tests. Permeability testing of the dynamically compacted crushed salt provided further evidence that the permeability decrease as the fraction density of the salt increases. The model predicted that stress

states exist where the radial strain rate would initially be positive (consolidation) and then reverse direction and become negative as the specimen density increases.

Ran et al. (1997) study the dynamic compaction properties of bentonite. The objective of the study is to determine the properties of bentonite seal and to evaluate the method of dynamic compaction for an effective bentonite shaft seal. Results of the dynamic compaction investigations delineate the influence of moisture content, compaction energy, mixed brine content, lift thickness, and rammer weight on the achievable dry density. Dynamic compactions can density bentonite to a dry density of 1.86 Mg/m^3 when mixed with WIPP brine and 1.74 Mg/m^3 when mixed with distilled deionized water. At these densities bentonite exhibits permeability on the order of $1.0 \times 10^{-19} \text{ m}^2$.

Cho et al. (2002) study the mechanical properties of compacted bentonite and bentonite-sand mixtures. The unconfined compression strength, young's modulus of elasticity, poisson's ratio, shear strength and consolidation properties of mixtures are collected and analyzed. The results show that the logarithm of unconfined compressive strength and young's modulus of elasticity increases linearly with increases dry densities, while decrease with increasing sand content. The shear strength increases with increasing dry densities.

Estabragh et al. (2013) study the mechanical behavior of compacted 20% bentonite and 80% kaolin mixture during wetting and drying cycles. The samples were inundated with different types of wetting fluids (distilled water, saline water and acidic water) swelling potential increases with an increasing number of wetting and drying cycles. The results show that the swelling potential increases with an increasing number of wetting and drying cycles. The effect of the distilled water on the swelling

potential is not the same as that of the saline water or the acidic water, acidic water and saline water in reducing the swelling potential of expansive soils.

Wang et al. (2014) propose to use compacted bentonite-based materials as possible sealing/backfill materials in deep geological repositories for high-level radioactive wastes (HLW) in several countries. Due to their favorable swelling characteristics, these materials are expected to fill up all voids left in the system after construction and emplacement of the waste packages. An important long-term safety function of bentonite-based barriers is to ensure a relatively impermeable zone around the high-level radioactive waste thereby limiting groundwater flow and waste package degradation rates and, ultimately, waste leaching rates. A mixture of bentonite and crushed Callovo-Oxfordian claystone was investigated. The long-term effect of pore water chemistry on the swelling pressure was studied at constant-volume conditions for 700 days. The results obtained in an initial period of 100 h revealed no significant influence of the water composition on the swelling pressure evolution, and the maximum swelling pressures observed were close to 4.30 MPa for a dry density of 1.70 Mg/m³. Over a longer time period, on the contrary, the swelling pressure eventually decreased for all samples, especially for the sample saturated with synthetic water. In addition, comparison of a one-step soaking test with a multi-step soaking test showed no wetting procedure effect on the long term swelling behavior.

Kaufhold et al. (2015) states that the swelling pressure of compacted bentonite may be affected by compaction/dry density after compaction (swelling pressure increases with increasing compaction), ionic strength (swelling pressure decreases with increasing salinity), initial water content (swelling pressure decreases with increasing water content), temperature and exchangeable cations (particularly at low dry density).

2.3 Direct Shear Test

Das (2008) states that the direct shear test is the oldest and simplest form of shear test arrangement. The direct shear test apparatus is shown in Figure 2.1. The test equipment consists of a metal shear box in which the soil specimen is placed. The soil specimens may be square or circular in plan. Normal force on the specimen is applied from the top of the shear box. Shear force is applied by moving one-half of shear box related to the other to cause failure in the soil specimen. Direct shear tests are repeated on similar specimens at various normal stresses. The normal stresses and the corresponding values, τ_f obtained from a number of tests are plotted on a graph from which the shear strength parameters are determined.

The resisting shear stress increases with shear displacement until a failure shear stress which is called the peak shear strength. After failure stress is attained, the resisting shear stress gradually decreases as shear displacement increases until it finally reaches a constant value called the residual shear strength or peak shear strength as shown in Figure 2.2. When approaching to the peak and residual shear strength, test results of specimen are based on Mohr-Coulomb Criterion.

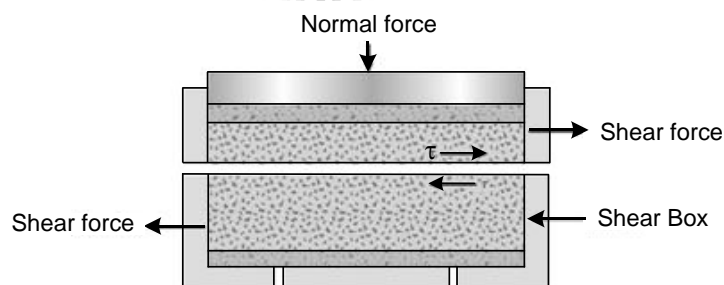


Figure 2.1 Direct shear box (Das, 2010).

Mohr (1990) presented a theory for rupture in materials that contented that material fails because of a critical combination of normal stress and shearing stress and not from either maximum normal or shear stress alone. Thus, the functional relationship between normal stress and shear stress on a failure plane can be expressed in the following form:

$$\tau_f = c + \sigma_n \tan \phi \quad (2.1)$$

The equation is so called Mohr-Coulomb failure criterion as shown in Figure 2.3.

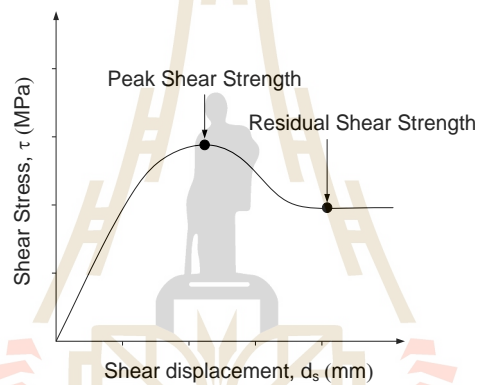


Figure 2.2 Nature of residual shear strength and peak shear strength (Das, 2010).

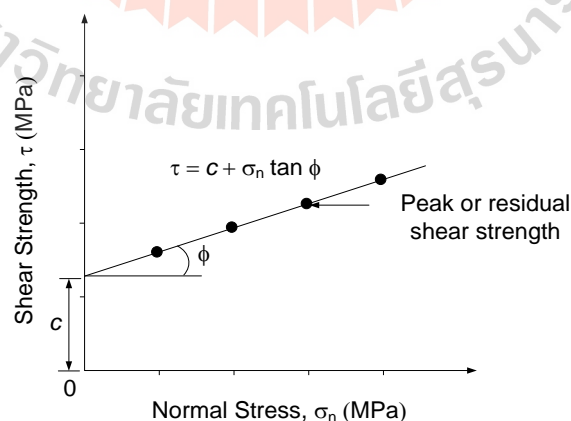


Figure 2.3 Mohr-Coulomb criterion as a function of shear strengths and normal stresses (Das, 2010).

Sonsakul et al. (2013) studied the performance assessment of three-ring compaction and direct shear testing device. The three-ring compaction and direct shear mold has been developed to obtain the optimum water content, dry density and shear strength of compacted soil samples. The device can shear the soil samples with grain size up to 10 mm. It can be used as a compaction mold and direct shear mold without removing the soil sample, and hence eliminating the sample disturbance. Commercial grade bentonite is tested to verify that the three-ring mold can provide the results comparable to those obtained from the ASTM standard testing devices. Three types of soil, including clayey sand, poorly-graded sand and well-graded sand, are tested to assess the performance of the device. Their results are compared with those obtained from the ASTM standard test device. The results indicate that the shear strength, maximum dry density and optimum water content of the bentonite obtained from the three-ring mold and the ASTM standard mold are virtually identical. The three-ring mold yields the higher maximum dry density than those obtained from the standard mold. The shear strengths obtained from the three-ring mod are also higher than those from the standard shear test device. This is primarily because the three-ring mold can accommodate the soil particles up to 10 mm for the shear test, and hence resulting in higher shear strengths that are closer to the actual behavior of the soil under in-situ conditions.

2.4 Laboratory Test

ASTM (D 1883) determines the final swell measurements and calculate the swell as a percentage of the initial height of the specimen. Apply weight on the mold in water allowing free access of water to the top and bottom of the specimen. Take

initial measurements for swell and allow the specimen to soak. Maintain a constant water level during this period. A shorter immersion period is permissible for fine grained soils or granular soils that take up moisture readily, if tests show that the shorter period does not affect the results.

ASTM (D422) determines the percentage of different grain sizes contained within a soil. The mechanical or sieve analysis can be performed to determine the distribution of the coarser, larger-sized particles, and the hydrometer method is used to determine the distribution of the finer particles. The distribution of different grain sizes affects the engineering properties of soil. Grain size analysis provides the grain size distribution, and it is required in classifying the soil.

ASTM (D854-00) determines the specific gravity of soil by using a pycnometer. Specific gravity is the ratio of the mass of unit volume of soil at a stated temperature to the mass of the same volume of gas-free distilled water at a stated temperature. The specific gravity of a soil is used in the phase relationship of air, water, and solids in a given volume of the soil.

ASTM (D1557) determines the relationship between the moisture content and the dry density of a soil for a specified compactive effort. The compactive effort is the amount of mechanical energy that is applied to the soil mass. Several different methods are used to compact soil in the field, and some examples include tamping, kneading, vibration, and static load compaction.

This laboratory will employ the tamping or impact compaction method using the type of equipment and methodology developed by R. R. Proctor (1933), therefore, the test is also known as the Proctor test. Two types of compaction tests are routinely performed: (1) the Standard Proctor test, and (2) the Modified Proctor test. In the

Standard Proctor test, the soil is compacted by a 5.5 lbs hammer falling a distance of one foot into a soil filled mold. The mold is filled with three equal layers of soil, and each layer is subjected to 25 drops of the hammer. The Modified Proctor test is identical to the Standard Proctor test except it employs, a 10 lbs hammer falling a distance of 18 inches, and uses five equal layers of soil instead of three. There are two types of compaction molds used for testing. The smaller type is 4 inches in diameter and has a volume of about $1/30 \text{ ft}^3$ (944 cm^3), and the larger type is 6 inches in diameter and has a volume of about $1/13.333 \text{ ft}^3$ ($2,123 \text{ cm}^3$). If the larger mold is used each soil layer must receive 56 blows instead of 25 (Table 2.1).

The soil sample is compacted with various water contents in lower ring mold. After several compactions for each water contents, the moist unit weight of compacted soil (γ) is calculated as followed equation (2.2):

$$\gamma = \frac{W}{V_m} \quad (2.2)$$

where W is weight of compacted soil and V_m is volume of the mold (lower ring).

From each moist dry density, the dry density of soil can be calculated by substituting the individual moisture content of those moist dry densities in the following equation (2.3):

$$\gamma_d = \frac{\gamma}{1 + \frac{w(\%)}{100}} \quad (2.3)$$

where γ_d is the dry unit weight of soil sample and w is the individual water content of

Table 2.1 Alternative Proctor Test Methods (Reddy, 2005)

	Standard Proctor ASTM 698			Modified Proctor ASTM 1557		
	Method A	Method B	Method C	Method A	Method B	Method C
Material	≤ 20% Retained on No.4 Sieve	>20% Retained on No.4 Sieve ≤ 20% Retained on 3/8" Sieve	>20% Retained on No.3/8" <30% Retained on 3/4" Sieve	≤ 20% Retained on No.4 Sieve	>20% Retained on No.4 Sieve ≤ 20% Retained on 3/8" Sieve	>20% Retained on No.3/8" <30% Retained on 3/4" Sieve
For test sample, use soil passing	Sieve No.4	3/8" Sieve	3/4" Sieve	Sieve No.4	3/8" Sieve	3/4" Sieve
Mold	4" DIA	4" DIA	6" DIA	4" DIA	4" DIA	6" DIA
No. of layers	3	3	3	5	5	5
No. of blows/layer	25	25	56	25	25	56

Note: Volume of 4 inches of diameter mold = 944 cm³, Volume of 6 inches of diameter mold = 2123 cm³ (verify these values prior to testing).

moist unit weight. After repeated compaction tests on various water contents, the compaction curve is drawn through individual water content and each dry density as shown in Figure 2.4.

ASTM (D4318) determines the plastic and liquid limits of a fine grained soil. The liquid limit (LL) is arbitrarily defined as the water content, in percent, at which a pat of soil in a standard cup and cut by a groove of standard dimensions will flow together at the base of the groove for a distance of 13 mm (1/2 in.) when subjected to 25 shocks from the cup being dropped 10 mm in a standard liquid limit apparatus

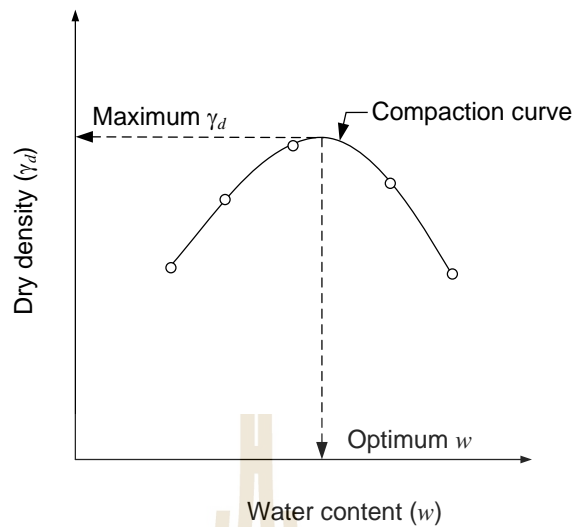


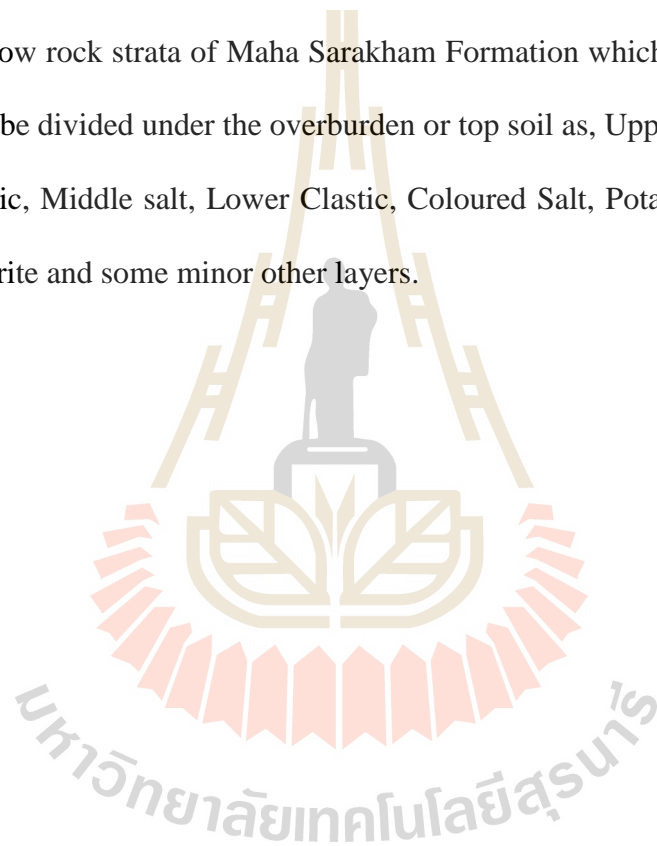
Figure 2.4 Proctor compaction test result (Proctor, 1933).

operated at a rate of two shocks per second. The plastic limit (PL) is the water content, in percent, at which a soil can no longer be deformed by rolling into 3.2 mm (1/8 in.) diameter threads without crumbling. The plastic limit is the moisture content that defines where the soil changes from a semi-solid to a plastic (flexible) state. The liquid limit is the moisture content that defines where the soil changes from a plastic to a viscous fluid state. The shrinkage limit is the moisture content that defines where the soil volume will not reduce further if the moisture content is reduced. A wide variety of soil engineering properties have been correlated to the liquid and plastic limits, and these Atterberg limits are also used to classify a fine-grained soil according to the Unified Soil Classification system or AASHTO system.

2.5 Numerical simulations

FLAC developed by Itasca Consulting Group Inc. (1992). FLAC is a two-dimensional explicit finite difference program for engineering mechanics computation.

This program simulates the behavior of structures built of soil, rock, or other materials that may undergo plastic flow when their yield limits are reached. Materials are represented by elements, or zones, that form a grid that is adjusted by the user to fit the shape of the object to be modeled. The Department of mineral Resource classified and interpreted data of salt and potash in northeastern Thailand for study and compare the total boreholes which had been drilled as many as 194 drill holes from 1973 to 1982. The result show rock strata of Maha Sarakham Formation which mostly composed of rock salt can be divided under the overburden or top soil as, Upper Clastic, Upper salt, Middle Clastic, Middle salt, Lower Clastic, Coloured Salt, Potash Zone, Lower Salt, Basal Anhydrite and some minor other layers.



CHAPTER III

SAMPLE PREPARATIONS

3.1 Introduction

This chapter describes basic characteristics of materials tested in this study. The materials consist of bentonite, crushed salt and saturated bine.

3.2 Sample preparation

3.2.1 Bentonite

Bentonite used in this study is from Thai Nippon Chemical Industry Co., LTD, Thailand (Figure 3.1). Tables 3.1 and 3.2 show the basic properties and the chemical compositions of bentonite in this study. The bentonite has initial water content of 8-12%. The liquid limit (LL), plastic limit (PL), plasticity index (PI) and specific gravity are determined according to ASTM D4318-05, D854-00 and D422-07. The chemical compositions are determined by X-Ray Fluorescence (XRF) Energy Dispersive Spectrometer Model XGT-5200. The results are reported based on 100% normalization of oxide compounds.

3.2.1.1 Initial water content of air-dried bentonite

The initial water content or natural water content is one of the most significant index properties used in establishing a correlation between bentonite behavior and its index properties. The test method is a determination of the water (moisture) content in the laboratory by weight of soil and rock which are most

applicable. The test method is performing according to ASTM D2216. The test specimen is dried in an oven at a temperature of $90^{\circ}\pm 5^{\circ}\text{C}$ to a constant mass. The loss of mass due to drying is considered to be water. The water content is calculated using the mass of water and the mass of the dry specimen.

3.2.1.2 Specific gravity

The test method covers the determination of the specific gravity of soil solids that pass the 4.75 mm (No. 4) sieve, and to understand a general way to find specific gravity of substance greater than one, which composes of small particles. The test method is conducted in accordance with ASTM D854. For the determination of specific gravity, the air dried soil about 50 grams is placed in a pycnometer. The pycnometer is heated on hot plate. After heating, more water is filled into the pycnometer until reaching the standard mark on the neck of pycnometer. The temperature decreasing based on time and the weight of pycnometer are recorded. After the decreasing temperature is reached under 30°C , the recording is stopped and all mixtures are taken out of the pycnometer to dry in the oven. To determine the specific gravity of soil solid, weight of oven dried soil is multiplied by temperature correction factor.

3.2.1.3 Atterberg's limit

Atterberg's limit test carries out to determine plastic limit (PL), liquid limit (LL) and plasticity index (PI) of bentonite. The test method follows ASTM D4318. The liquid limit is prepared by set of liquid limit device. The set includes a brass cup, grooving tool, and dropping cup machine. The bentonite sample is prepared in brass cup where the soil is placed a part of soil in standard cup and cut by a groove of standard dimensions. The groove width is 13 mm (about 1/2 in) and the brass cup is

dropped from 10-mm by apparatus operating with a rate of two shocks per second. When the groove is closed each other of sides, the sample is taken to dry in the oven and the number of dropped shocks is recorded. Repeated manner is at least three times between 15 shocks and 25 shocks. The liquid limit is determined the water content at the 25 shocks to be closer the each side of groove of brass cup. The plastic limit is the water content at which the sample cannot be longer by deformation with a thread diameter about 3.2 mm (1/8 in) without crumbling.

3.2.2 Crushed salt

Crushed salt used in this study is prepared from the Middle member of the Maha Sarakham Formation in the Korat basin, Thailand. The salt was donated by Asean Potash Mining Co., Ltd (APMC). The crushed salt is passing through sieve number 4, 8, 18, 40, 60, 100, 140 and 200. They are crushed by hammer mill (2HP-4 POLES, Spec jis c-4004) to obtain grain size ranging from 0.075 to 2.35 mm (Figure 3.2). The grain size distribution curve show in Figure 3.3. Table 3.3 shows chemical compositions of crushed salt was determined by X-Ray Fluorescence (XRF) Energy Dispersive Spectrometer Model XGT-5200 (Khamrat, 2016).

Table 3.1 Engineering basic properties of bentonite.

Property	Bentonite
Liquid limit, (%)	357
Plastic limit, (%)	44
Plasticity index, (%)	313
Specific gravity	2.50
Moisture content, (%)	8-12
Dry particle size	80% pass through 200 mesh

3.2.3 Saturated brine

Saturated brine is prepared from pure salt (NaCl) 2.7 kg with distilled water in plastic tank and stirred by a plastic stick continuously for 20 minutes. The proportion of salt to water is about 39% by weight. The specific gravity of the saturated brine in this study is 1.21 at 21°C. The specific gravity of saturated brine can be calculated by:

$$SG_{\text{Brine}} = \frac{\rho_{\text{Brine}}}{\rho_{\text{H}_2\text{O}}} \quad (3.1)$$

where SG_{Brine} is specific gravity of saturated brine

ρ_{Brine} is density of saturated brine (measured with a hydrometer (kg/m^3))

$\rho_{\text{H}_2\text{O}}$ is density of water equal $1,000 \text{ kg}/\text{m}^3$

3.2.4 Bentonite and crushed salt mixtures.

The bentonite-crushed salt mixture is a combination of two different materials Bentonite (B) and crushed salt (S) mixture ratios of 100:0, 90:10, 80:20, 70:30, 60:40, 50:50, 40:60, 30:70, 20:80 and 10:90 by weight are mixed with saturated brine at 0, 5, 10, 15, 20, 25, 30, 35 and 40% by weight. The mixtures are prepared using plastic spatula with 2,500 kilogram of total weight. The brine is added by spaying on the mixtures (Figure 3.4). The mixtures are compacted in the three-ring mold.



Figure 3.1 Bentonite obtained from Thai Nippon Chemical Industry Co., LTD, Thailand.

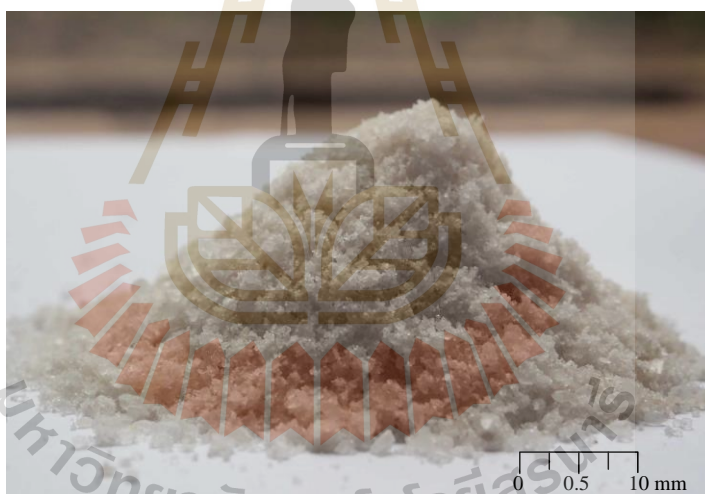


Figure 3.2 Crushed salt from a hammer mill machine.

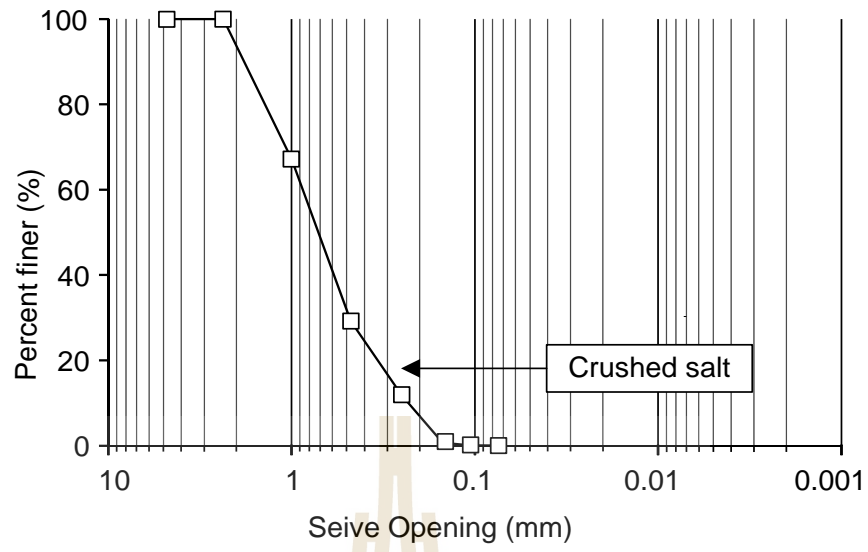


Figure 3.3 Grain size distribution of crushed salt.



Figure 3.4 Bentonite and crushed salt are mixes with saturated brine.

Table 3.2 Typical chemical compositions of bentonite.

Compositions	Concentration (% weight)	
	Bentonite	Bentonite (Sonsakul et al., 2013)
SiO ₂	56.99	61.93
Al ₂ O ₃	15.43	19.85
Fe ₂ O ₃	14.16	4.45
Na ₂ O	-	1.63
MgO	5.4	2.44
CaO	4.26	1.27
K ₂ O	0.57	0.44
TiO ₂	2.74	0.19
SO ₃	0.17	1.27
SrO	0.06	0.03
ZrO ₂	0.03	0.03
ZnO	0.02	-
MnO ₂	0.18	0.02
Total	100	100

Table 3.3 Chemical compositions of crushed salt obtained by XRF analysis

(Khamrat, 2016).

Oxides	Percentage weight
Na ₂ O	20.70
MgO	4.39
Al ₂ O ₃	N/D
SiO ₂	0.03
SO ₃	0.05
Cl ₂ O	68.03
K ₂ O	6.40
CaO	0.26
Fe ₂ O ₃	N/D
Br ₂ O	0.16
SrO	N/D
Total	100

CHAPTER IV

TEST METHOD AND RESULTS

4.1 Introduction

This chapter describes the test equipment, methods and results of the compaction and direct shear testing. The swelling capacity and loading are measured under saturated condition and under cycles of wet-dry conditions. Using compaction tests are also performed to obtain the parameters for computer simulations.

4.2 Test Equipment for Compaction and Direct Shear Tests

Sonsakul and Fuenkajorn (2013) present the three-ring compaction and direct shear mold which has been developed to determine the optimum water content, maximum dry density and shear strength of compacted soil samples with particle sizes up to 10 mm. It is designed to be used as a compaction mold and direct shear mold without removing the soil sample, and hence eliminating the sample disturbance. The results indicate that the shear strength, maximum dry density and optimum water content of the bentonite obtained from the three-ring mold and the ASTM standard mold are virtually identical.

The three rings compaction molds (Figure 4.1a) are secured on the base plate using steel bolts and two steel clamps. These clamps are removed when the mold is placed into a direct shear load frame, and hence they can be displaced (sheared) when the lateral force is applied during shear test.

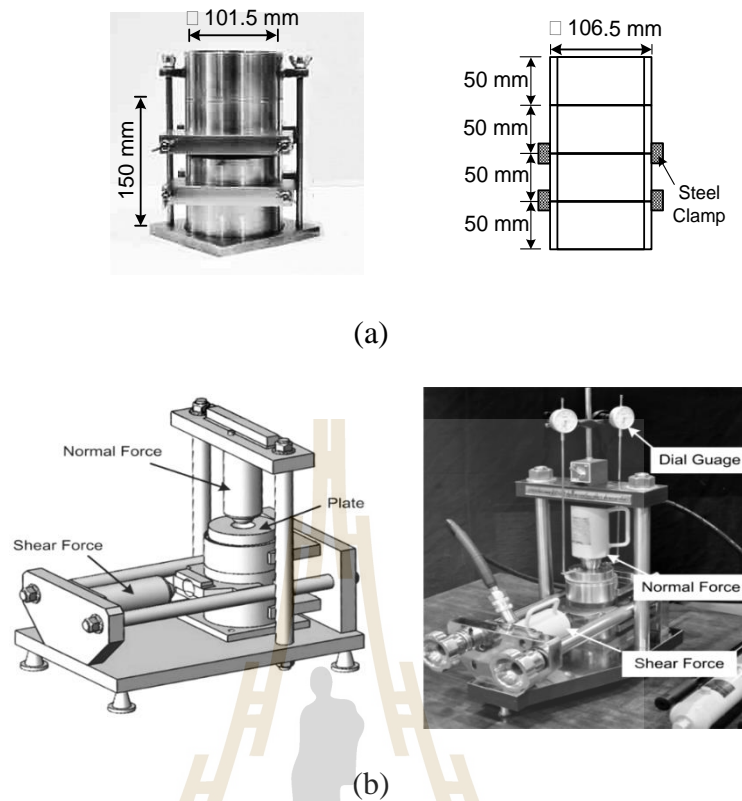


Figure 4.1 Three-ring compaction mold (a) and direct shear test frame developed for use with the three-ring mold (b) (Sonsakul and Fuenkajorn, 2013).

The main components for the shear test frame are the lateral load system for pushing the middle ring, and the vertical load system for applying a constant normal stress on the compacted soil sample (Figure 4.1b).

4.3 Compaction Test Method and Results

The objectives of these tests are to determine the optimum brine content and maximum dry density of bentonite-crushed salt mixtures. The mixtures are compacted in the three-ring compaction mold (Sonsakul and Fuenkajorn, 2013). They are mixed with the saturated brine varying from 0 to 35%. The modified proctor method are uses

in this sections. The mixtures are compacted with a release of weight steel hammer 10 pounds in mold of 27 times per layer in 6 layers. Total energy of modified compaction is $2,700 \text{ kN}\cdot\text{m}/\text{m}^3$. Energy of compaction (J) can be calculated by (Proctor, 1933):

$$J = \frac{n \times W \times L \times t}{V} \quad (4.1)$$

where J is compaction energy per unit volume, n is number of blows per layer, W is weight of hammer, L is height of drop of hammer, t is number of layers and V is volume of mold.

The dry densities and brine contents are plotted to determine the maximum dry density and optimum brine content (Figure 4.2). The brine content (W_B) can be calculated by (Fuenkajorn, 1988):

$$W_B = \frac{[100 + S_B] \times [W_1 - W_2 - (\frac{W_i}{100})(W_2 - W_{can})] \times 100}{100 \times (W_2 - W_{can}) - S_B(W_1 - W_2)} \quad (4.2)$$

where W_B is brine content (%),

W_i is initial water content of specimen (%)

W_{can} is weight of container (g)

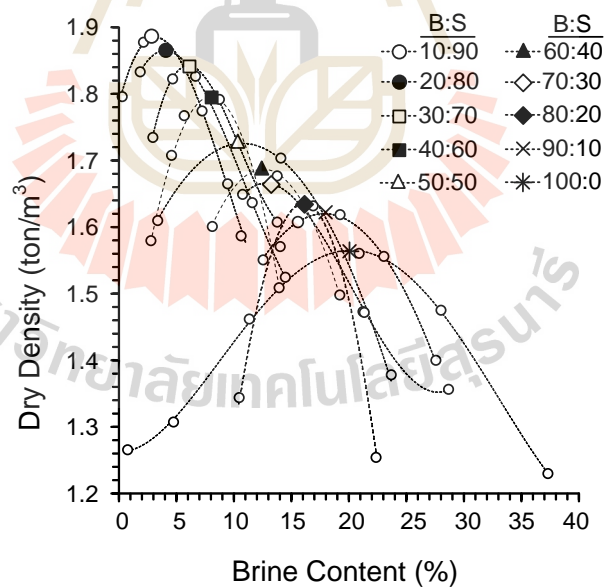
W_1 is weight of wet soil and container (g)

W_2 is weight dry soil and container (g)

and S_B is solubility of salt in dissolved water (%).

Table 4.1 Compaction test results.

Bentonite (B): Crushed salt (S)	Optimum brine content (%)	Maximum dry density (ton/m ³)
90:10	18.0	1.62
80:20	16.0	1.64
70:30	13.0	1.67
60:40	12.2	1.69
50:50	10.0	1.73
40:60	7.9	1.80
30:70	6.0	1.84
20:80	4.0	1.87
10:90	2.8	1.89

**Figure 4.2** Relationship between dry density and brine content as function of bentonite content.

Results indicate that the maximum dry density increases with decreasing bentonite content (%) and the optimum brine content increases with increasing bentonite content (%). The results of the compaction test are summarized in Table 4.1. This agrees with the results obtained by Akgun et al. (2015).

4.4 Direct Shear Test Method and Results

The direct shear test is performed to determine maximum shear strengths of the mixtures with the optimum brine content after compacted in the three ring mold. After the mixtures are compacted, the steel clamps are removed when the mold is placed into a direct shear load frame (Figure 4.3).

The main components for the shear test frame are the lateral load system for pushing the middle ring and the vertical load system for applying a constant normal load on the compacted sample. Normal stresses used are 0.1, 0.2, 0.4, 0.6, 0.8 and 1 MPa. The normal and shear force are applied by a hydraulic load cell. The shear stress is applied while the shear displacement and dilation are observed for every 0.1 mm of shear displacement. The normal stress and shear stress can calculate from the equations:

$$\sigma_n = \frac{P}{A} \quad (4.3)$$

$$\tau = \frac{F}{2A} \quad (4.4)$$

where σ_n is normal stress, P is normal load, A is cross section area of sample, F is shear force and τ is shear stress. The peak shear strength is used to calculate the cohesion and friction angle. It can be expressed as:

$$\tau = c + \sigma \tan \phi \quad (4.5)$$

where τ and σ are the shear stress and normal stress, ϕ is the angle of internal friction, and c is cohesion. The results are shown in the form of the Coulomb's criterion. The shear stresses as a function of shear displacement are shown in Figure 4.4. The shear stresses increase with shearing displacement, particularly under high normal stresses. Figure 4.5 shows peak shear stresses as a function of normal stresses. Figure 4.6 and Figure 4.7 shows the friction angle and cohesion as a function of bentonite content. Table 4.2 shows the cohesion and friction angle obtained from the direct shear testing. The higher shear strength is obtained from the lower percentages of bentonite mixtures. Results indicate that the shear strength increase with increasing crushed salt content.

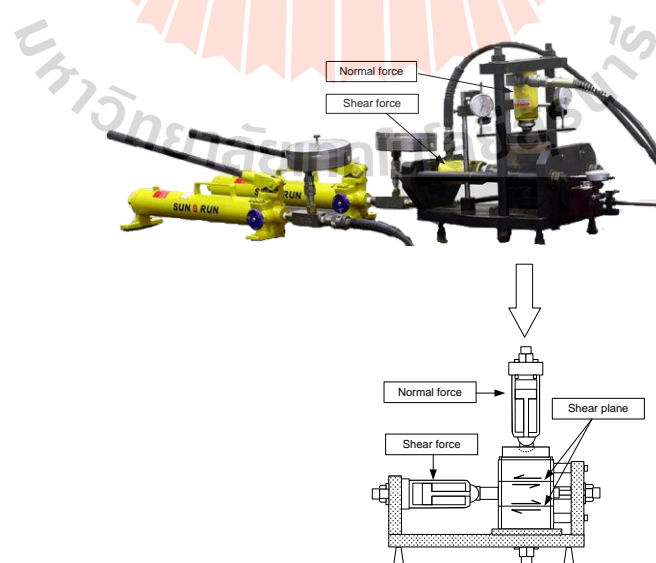


Figure 4.3 Three ring mold in the direct shear frame.

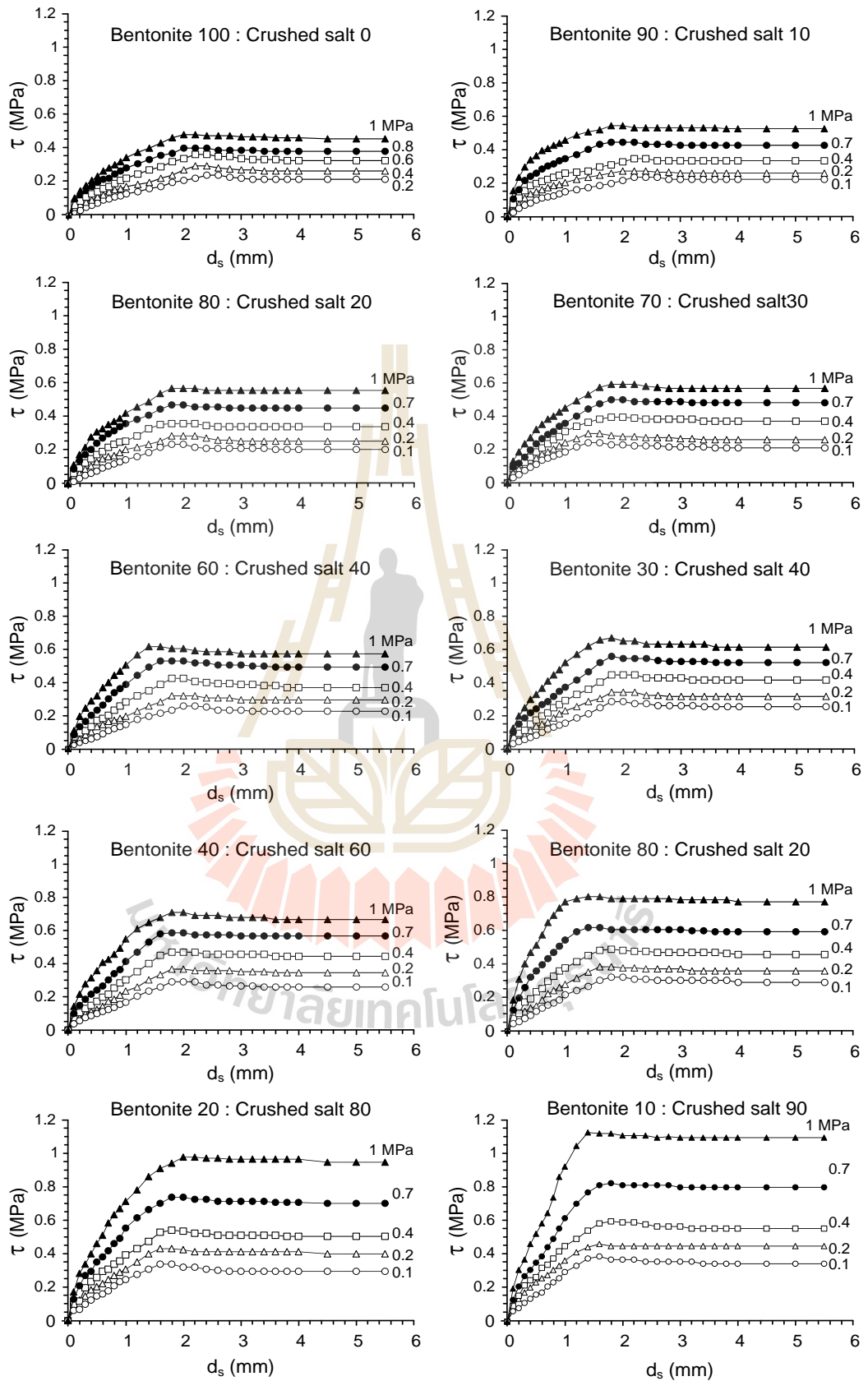


Figure 4.4 Shear stresses as a function of shear displacement.

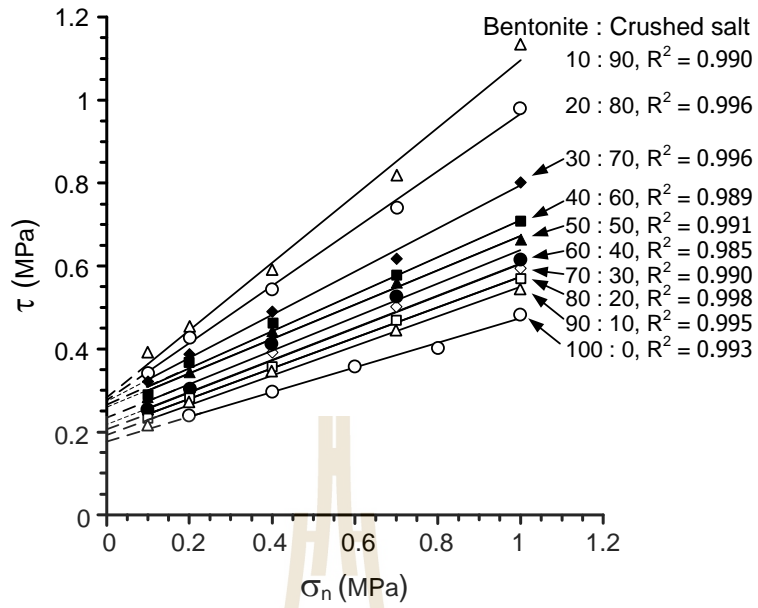


Figure 4.5 Shear strength as a function of normal stress.

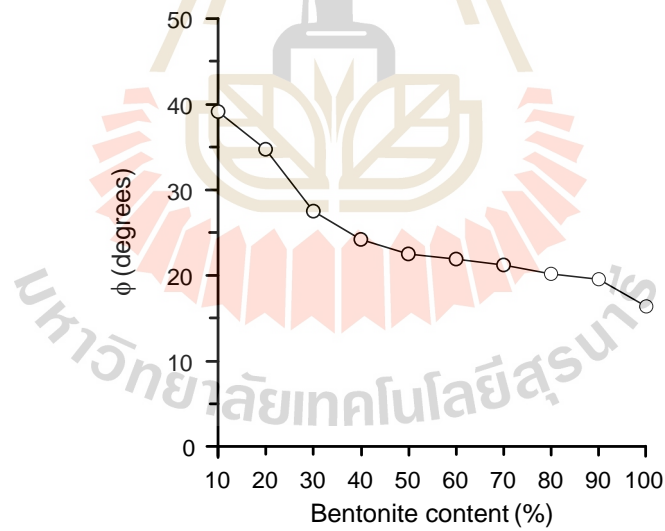
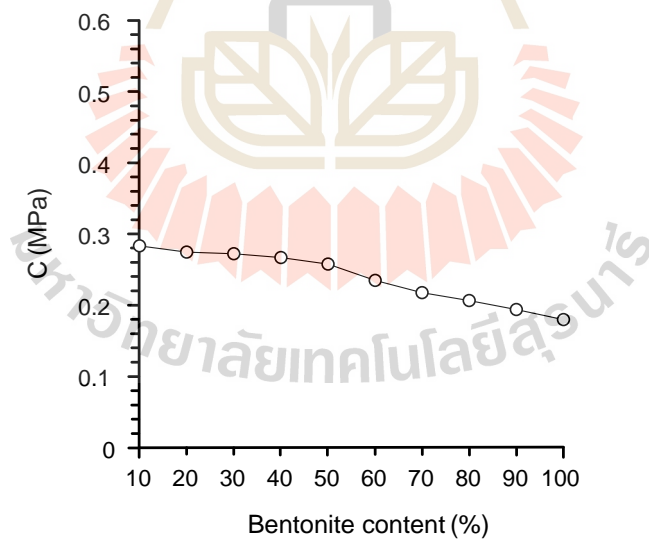


Figure 4.6 Friction angle as a function of bentonite content.

Table 4.2 Direct shear test results.

Bentonite (B): Crushed salt (S)	c (kPa)	ϕ (degrees)	R ²
100:0	180	16	0.993
90:10	194	20	0.995
80:20	207	20	0.998
70:30	218	21	0.990
60:40	235	22	0.985
50:50	258	22	0.991
40:60	267	24	0.989
30:70	273	27	0.996
20:80	275	35	0.996
10:90	284	39	0.990

**Figure 4.7** Cohesion as a function of bentonite content.

4.5 Swelling Test Method and Results

The bentonite is mixed with the crushed salt under the ratios of bentonite-to-crushed salt from 40:60, 50:50, 60:40, 80:20 and 100:0. Each sample is compacted in the three rings mold for 27 times, in six layers. After compaction procedure, remove the cover mold test and trimmed the top of the surface is smooth. The sand (porous media) is added to replace the removed sample and insert the acrylic sheet at the top of the sample. The measurements of swelling are recorded every five minutes by a displacement dial gage (Figure 4.8). The swelling is calculated by:

$$D = \left(\frac{\Delta H}{H} \right) \times 100 \quad (4.6)$$

where D is swelling ratio (%), H is the initial height and ΔH is the change of the height. Figure 4.9 shows swelling ratio results measured as a function of time. The compacted bentonite-crushed salt mixture of 100:0 shows the swelling nearly 14% after 15 days. The swelling ratio of all mixtures are rapidly increased and reaching its peak within 3 days after that it continues with little fluctuation except for the samples with of 100:0 and 80:20. They fluctuate until 15 days and tend to remain constant. The results indicate that the swelling ratio increase with increasing bentonite content.

4.5.1 Wet-Dry Cycles Test Method and Results

After swelling of the compacted specimens is measured in cycle 1, the saturated specimens are dried by the oven at 70 °c till the weight reaches to stable. Then brine is always added on the specimen till 15 days under ambient temperature and get dried again (cycles 2). The vertical swelling deformations is measured every 10

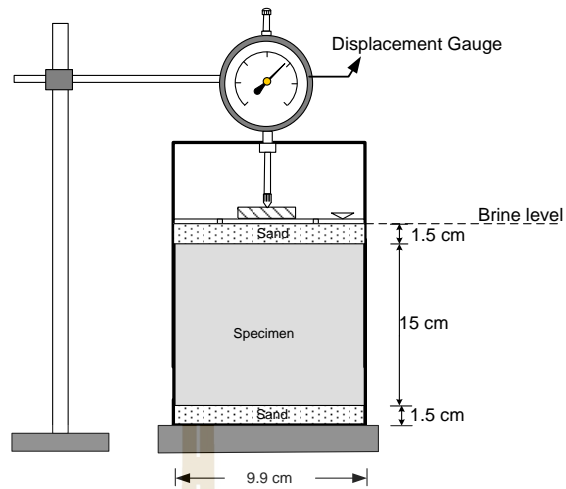


Figure 4.8 Swelling test in three-ring compaction mold.

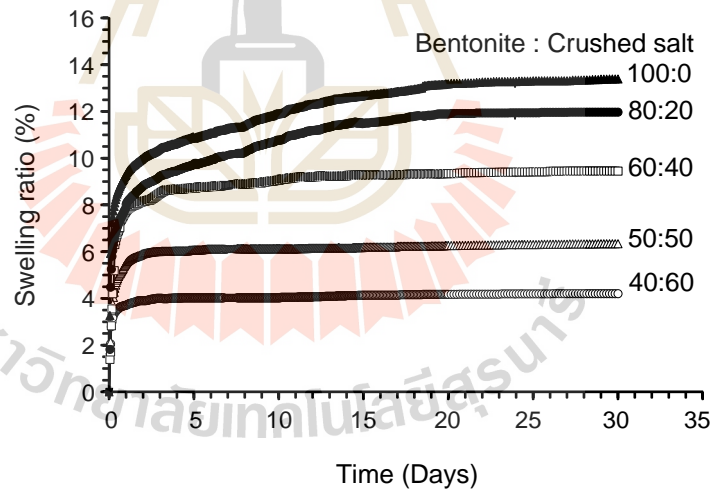


Figure 4.9 Swelling ratio as a function of time.

minutes. These procedure (wet and dry cycle) are repeated for 3 times (cycle 3). The results show that the swelling ratio increased with increasing bentonite content (Figure

4.10). The swelling of the specimens after get dried in cycle 2 tend to more increase particularly under higher bentonite contents. This is because the bentonite can absorb more brine and hence the specimen more swell. After the specimen is dried in cycle 3 however found that the swelling is slightly increasing. The swelling reaches constant after 3 days for all testing.

4.5.2 Swelling under Constant Loads Test Method and Results

The swelling deformations are also measured under static loads of 4.5, 9 and 13.5 kg. The test method is in accordance with the ASTM (D1883) standard practice. The brine is added to the specimen for 10 days. The swelling deformation ratio as a functions of time under 5, 9 and 13.5 kg loading condition is shown in Figure 4.11. Loading effects of compacted specimens on swelling ratio are presented in Figure 4.12. Results show that static load and bentonite content are important factor to control the swelling ratio. The swelling ratios increase with increasing static load and bentonite content.

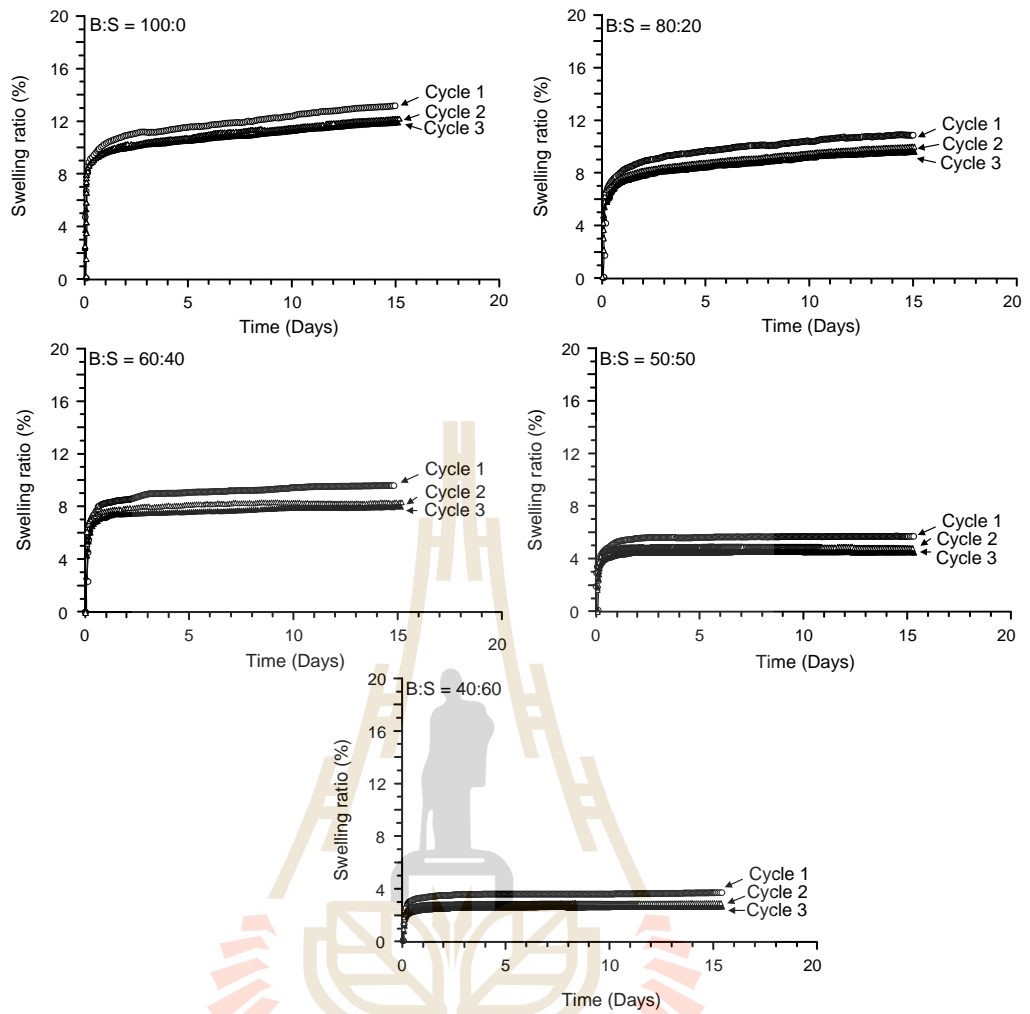
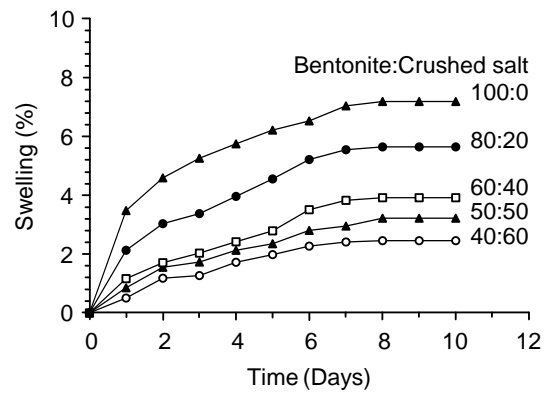
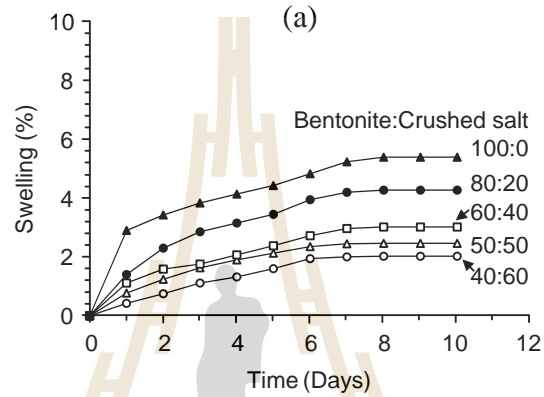


Figure 4.10 Swelling ratio as a function of time for 3 cycles.

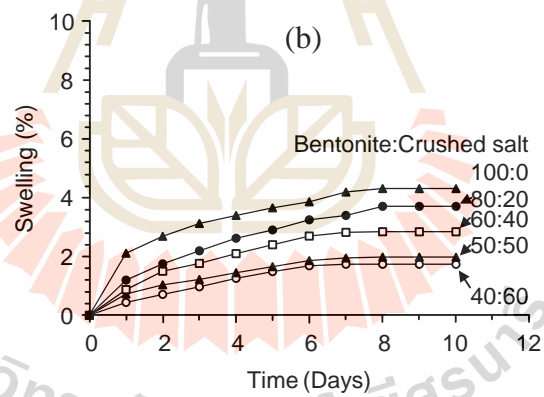
มหาวิทยาลัยเทคโนโลยีสุรนารี



(a)



(b)



(c)

Figure 4.11 Swelling ratio of bentonite-crushed salt mixtures as a function of time under load 4.5 kg (a), 9.0 kg (b) and 13.5 kg (c).

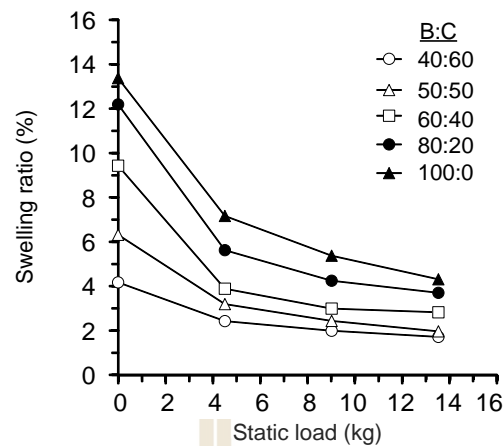


Figure 4.12 Swelling ratio of bentonite-crushed salt mixtures as a function of static load.

4.6 Uniaxial Compressive Strength Tests Method and Results

The uniaxial compressive strength test procedure follows as much as practical the ASTM (D2938-95) standard practice and the ISRM suggested method. The compressive strength is determined by axially loading the compacted bentonite-crushed salt mixture (after removing from the three ring mold) with a nominal diameter of 106.5 mm. Neoprene sheets are used to minimize the friction at the interfaces between the loading platens and the sample surfaces. The samples are loaded at the constant rate of 0.5-1 MPa/second until failure. The axial and lateral displacement is monitored by dial gages. The elastic modulus (E) and Poisson's ratio (ν) are determined from the tangent about 50% of the failure stress. Figure 4.13 shows all post-test specimen of bentonite-crushed salt mixture after uniaxial compressive strength testing. The results indicate that the uniaxial compressive strength and elastic modulus decrease with increasing bentonite content. The Poisson's ratios increase with increasing bentonite content. The results are shown in Figures 4.14.

Table 4.3 Uniaxial compressive strength results.

Materials	Elastic modulus (GPa)	Poisson's Ratio	Strength (MPa)
B:S = 40:60	0.84	0.10	0.79
B:S = 60:40	0.69	0.15	0.68
B:S = 80:20	0.45	0.18	0.64

**Figure 4.13** Post-tested bentonite-crushed salt mixture specimens after uniaxial compressive strength testing.

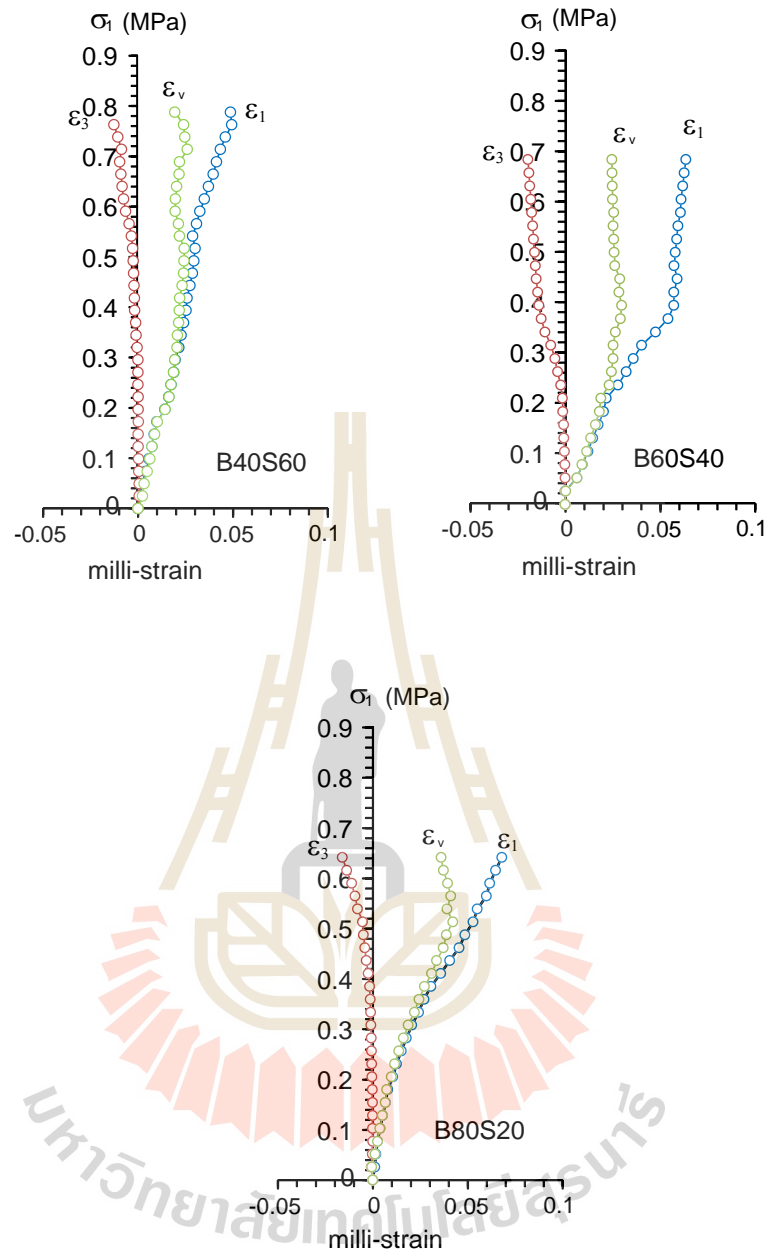


Figure 4.14 Uniaxial stress-strain curves of specimens.

CHAPTER V

COMPUTER SIMULATIONS

5.1 Introduction

The effects of overburden thickness, room height and bentonite contents on surface subsidence, and room and pillar deformation are investigated in this chapter. The FLAC 4.0 (Itasca, 1992) is used to determine the effectiveness of backfill in salt mines after the mine excavation is completed.

5.2 Input parameters

The stratigraphy of rock salt in Thailand has been compiled by many investigators (Japakasetr and Suwanich, 1977; Suwanich et al., 1982; Suwanich and Ratanajaruraks, 1986; Japakasetr, 1985). These data are obtained from the 194 exploration boreholes drilled in northeast of Thailand. In this study, the stratigraphic column of rock salt and clastic rock at Ban Hhao, Muang district, Udon Thani province (borehole no. K-089) is applied as an example for use in the computer simulations (Figure 5.1). The properties of the materials are shown in Tables 5.1 to 5.3. The salt property parameters are obtained from the calibration by Samsri et al. (2010) and Sriapai et al. (2012). The clastic rock properties are taken from Crosby (2007) and the compacted materials are obtained from this study. The simulated conditions include the clastic rock thickness varying from 200, 250 to 300 m with the constant rock salt thickness of 30 m. The room height is varied from 6, 8 and 10 m.

The mesh density is designed to simulate the overburden layer, rock salt layer and underground opening. There are over 700 elements covering the cross-section of the model. The x-axis is fixed on the left and right of boundaries, and the y-axis is fixed at the bottom boundary. The crushed salt emplacement gap about 30 cm between the roof and the top of backfill.

5.3 Simulation results

The computer simulations are calculated up to 50 years after backfill process. The surface subsidence, and roof, floor and pillar deformations under various overburden thickness and room heights are evaluated.

5.3.1 Duration before backfill

To study the effect of duration before backfill, the duration before backfill is varied from 6, 12 to 24 months. The overburden thickness is 200 m, room height is 6 m and salt thickness is 30 m. Figure 5.2 shows the finite difference mesh and boundary conditions. Figures 5.4 through 5.7 show the test results of opening deformations with bentonite-to-crushed salt (B:C) ratios of 80:20, 60:40 and 40:60. The computer simulation suggests that the duration before backfill slightly affects the deformations. The maximum surface subsidence is 14.69 cm for the duration before backfill of 24 months (Tables 5.4 through 5.8).

5.3.2 Opening height

The effect of opening height is investigated where the overburden thickness is constant at 300 m, the salt thickness is 30 m and duration before backfill is 24 months. The opening heights are varied from 6, 8 to 10 m (Figure 5.8). The surface subsidence and deformation of pillars and roofs under different opening heights are shown in

Figures 5.9 through 5.13. The maximum surface subsidence under no backfill is 21.98, 21.40 and 32.79 cm. Tables 5.4 through 5.8 show the deformation of surface subsidence, roof, floor and pillar deformations which increase with increasing opening height. The lower subsidence is observe for B:C = 40:60, ranging from 14.53 to 21.09 cm. The largest surface subsidence for B:C = 40:60 ranges from 19.99 to 25.75 cm.

5.3.3 Overburden thicknesses

The effect of overburden thickness is studied by varying the thickness from 200, 250 to 300 m, where the salt thickness is 30 m, opening height is 6 m and duration before backfill is 24 months. The finite difference mesh and boundary conditions are shown in Figure 5.14. The deformations after 50 years with backfill and without backfill conditions are shown in Figures 5.15 through 5.19. The computer simulation suggests that the deformation of surface subsidence, roof, floor and pillar deformations increase with increasing crushed salt contents and overburden thickness.

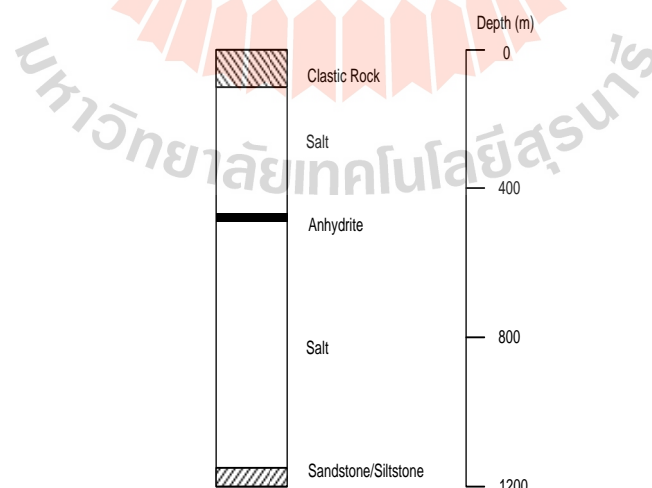


Figure 5.1 Stratigraphy of borehole no. K-089 at Ban Hhao, Muang district, Udon Thani province (Suwanich, 1986).

Table 5.1 Mechanical properties of clastic rock and rock salt for FLAC 4.0 simulations

(Crosby 2007, Sriapai et al, 2012).

Parameters	Rock types	
	Clastic rock	Rock salt
Density, ρ (kg/m ³)	2,490	2,150
Bulk modulus, K (GPa)	1.70	2.22
Shear modulus, G (GPa)	0.30	1.67
Cohesion, c (MPa)	3.50	0.50
Internal friction angle, ϕ (Degrees)	25	50
Tension, T (MPa)	0.83	1.00

Table 5.2 Time-dependent properties of rock salt for FLAC 4.0 simulations (Samsri et

al., 2010).

Parameters	Values
Elastic modulus, E_1 (GPa)	1.90
Spring constant in visco-elastic phase, E_2 (GPa)	5.79
Visco-plastic coefficient in steady-state phase, η_1 (GPa.day)	0.34
Viscon-plastic coefficient in transient phase, η_2 (GPa.day)	0.71
Density, γ (kg/m ³)	2,200

The largest surface subsidence is observed for the case of without backfill which ranges from 14.69 to 18.24 cm. The results are shown in Tables 5.4 through 5.8.

Table 5.3 Compacted material properties for FLAC 4.0 simulations.

Bentonite-to-crushed salt ratios (B:C)	Properties				
	Density (kg/m ³)	Elastic modulus (GPa)	Poisson's ratios	Cohesion (kPa)	Friction angle (degrees)
40 : 60	1,800	2.35	0.105	267	24
60 : 40	1,690	2.10	0.087	235	22
80 : 20	1,640	1.70	0.080	207	20

5.4 Discussions

The results obtained from the computer simulations show the surface subsidence and room and pillar deformations. Room and pillar deformations increase with increasing opening height and overburden thickness because in-situ stress increases with increasing overburden thickness (Newman and Zipf, 2005; Liu, 2011).

Figures 5.20 through 5.24 show the reduction of the surface subsidence and room and pillar deformations. The reductions of subsidence and opening deformations decrease with increasing B:C ratios. The results show that the compacted bentonite to crushed salt mixture can be applied in salt and potash mining to reduce the deformation of surface subsidence and room and pillar deformations, especially when room is very high. The lower bentonite content specimen has higher mechanical properties (uniaxial strength, elastic modulus, Poisson's ratio, friction angle and cohesion). Increasing crushed salt content increases the mechanical properties of the bentonite-crushed salt mixtures. This agrees with the results obtained by Butcher (1991) and Pfeifle (1991).

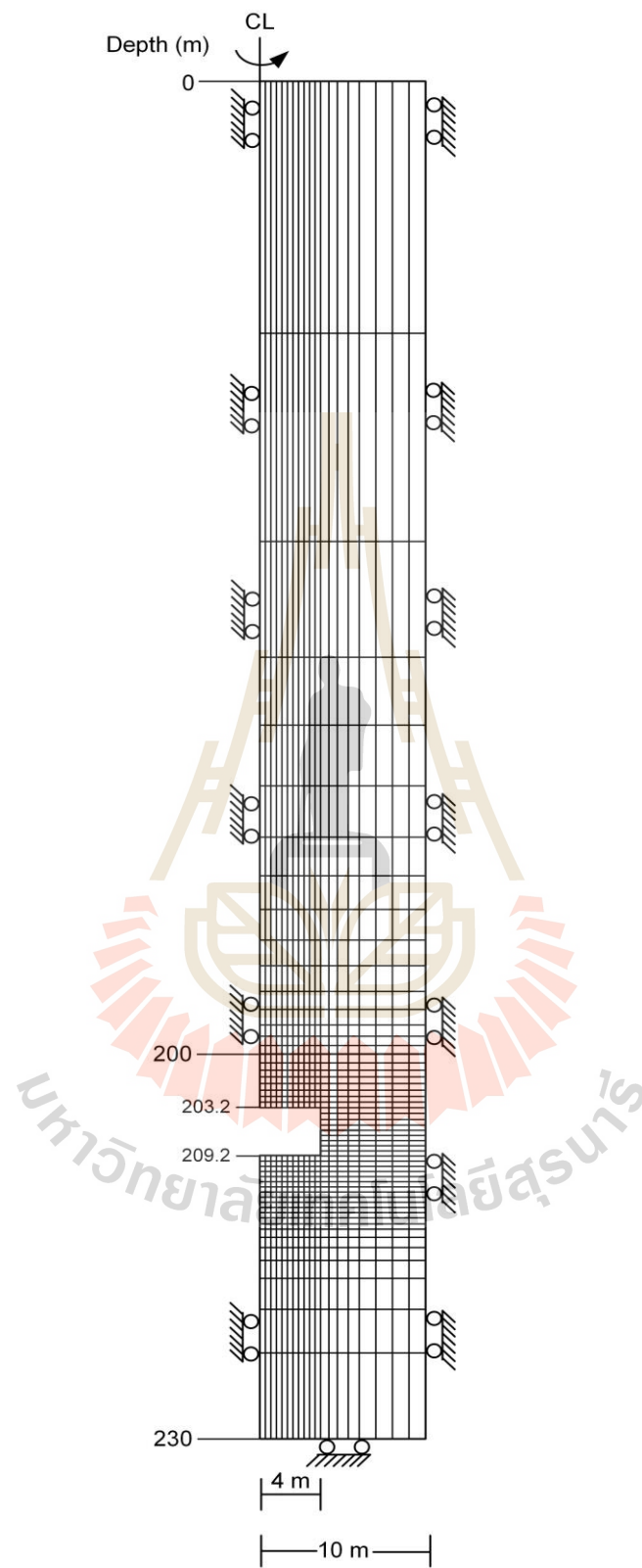


Figure 5.2 Mesh and boundary conditions used in this study.

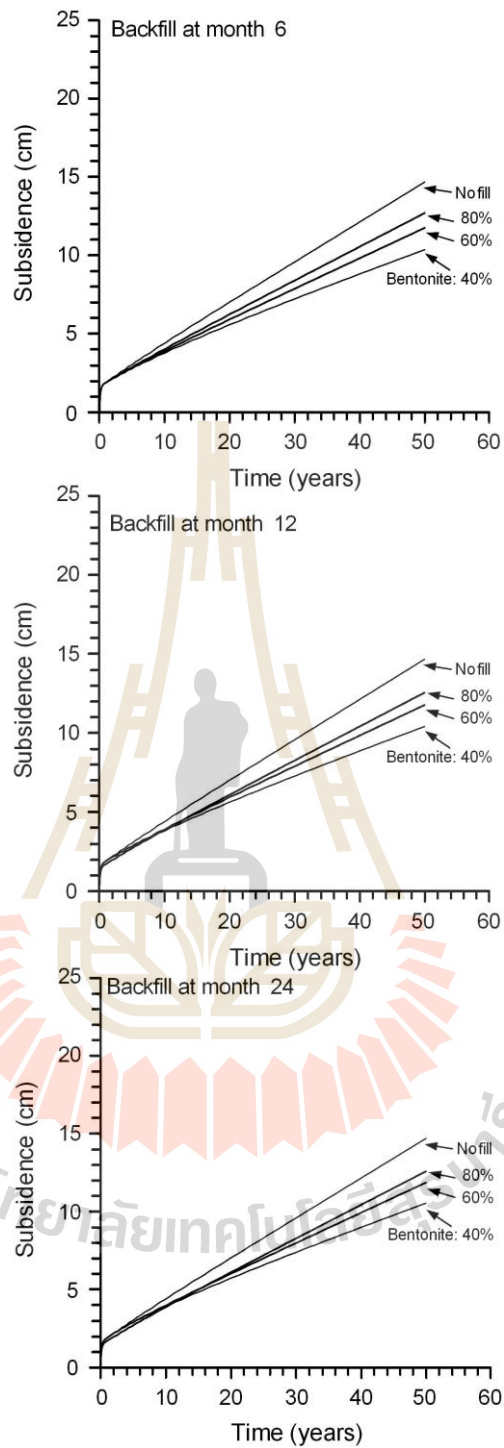


Figure 5.3 Surface subsidence as a function of time with different B:C ratios where overburden thicknesses 200 m, duration before backfill 6, 12 and 24 months, and opening height 6 m.

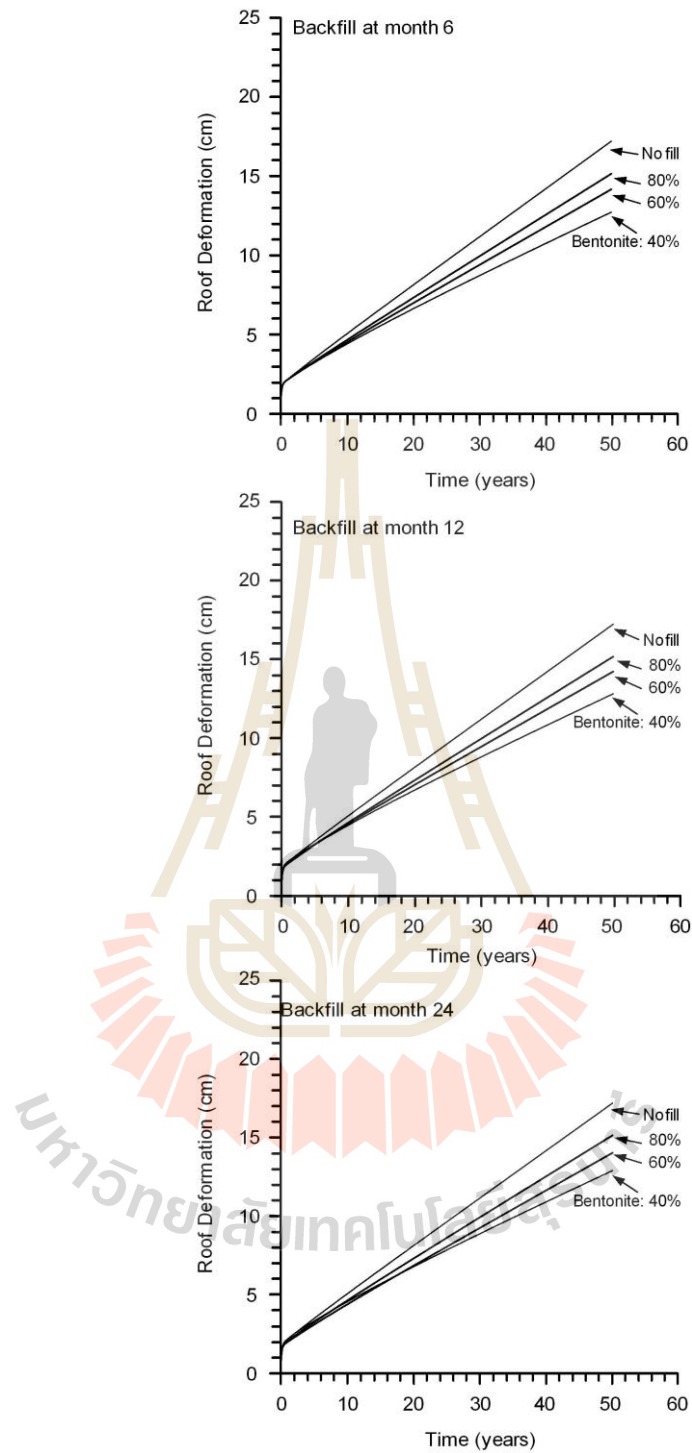


Figure 5.4 Roof deformation as a function of time with different B:C ratios where overburden thicknesses 200 m, duration before backfill 6, 12 and 24 months, and opening height 6 m.

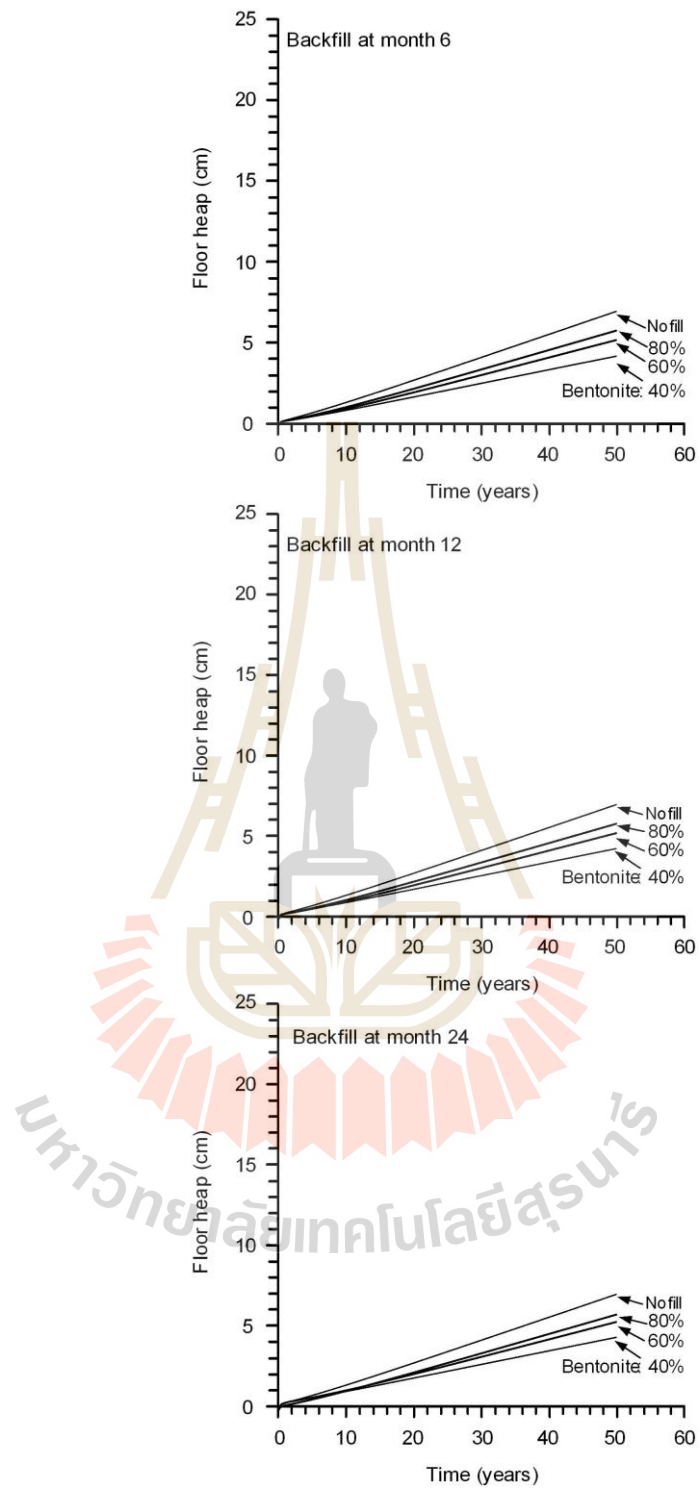


Figure 5.5 Floor heap as a function of time with different B:C ratios where overburden thicknesses 200 m, duration before backfill 6, 12 and 24 months, and opening height 6 m.

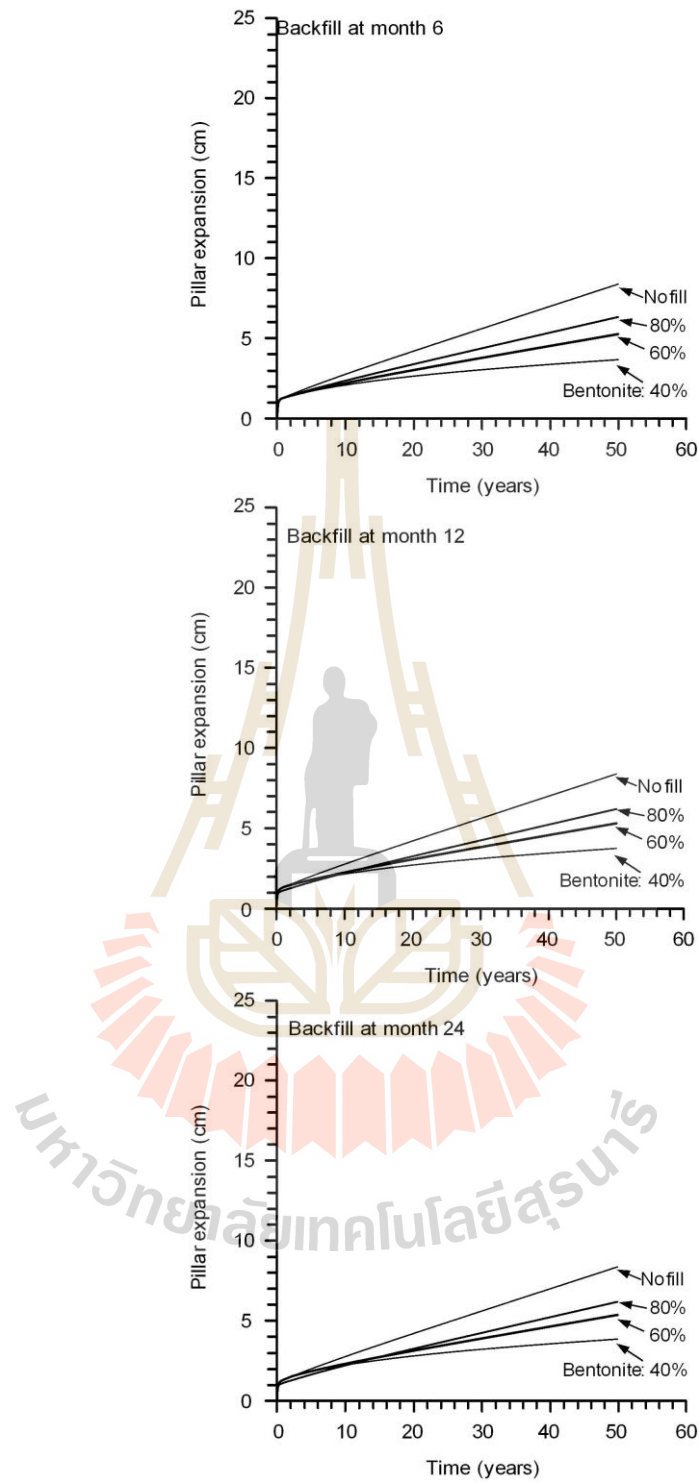


Figure 5.6 Pillar expansion as a function of time with different B:C ratios where overburden thicknesses 200 m, duration before backfill 6, 12 and 24 months, and opening height 6 m.

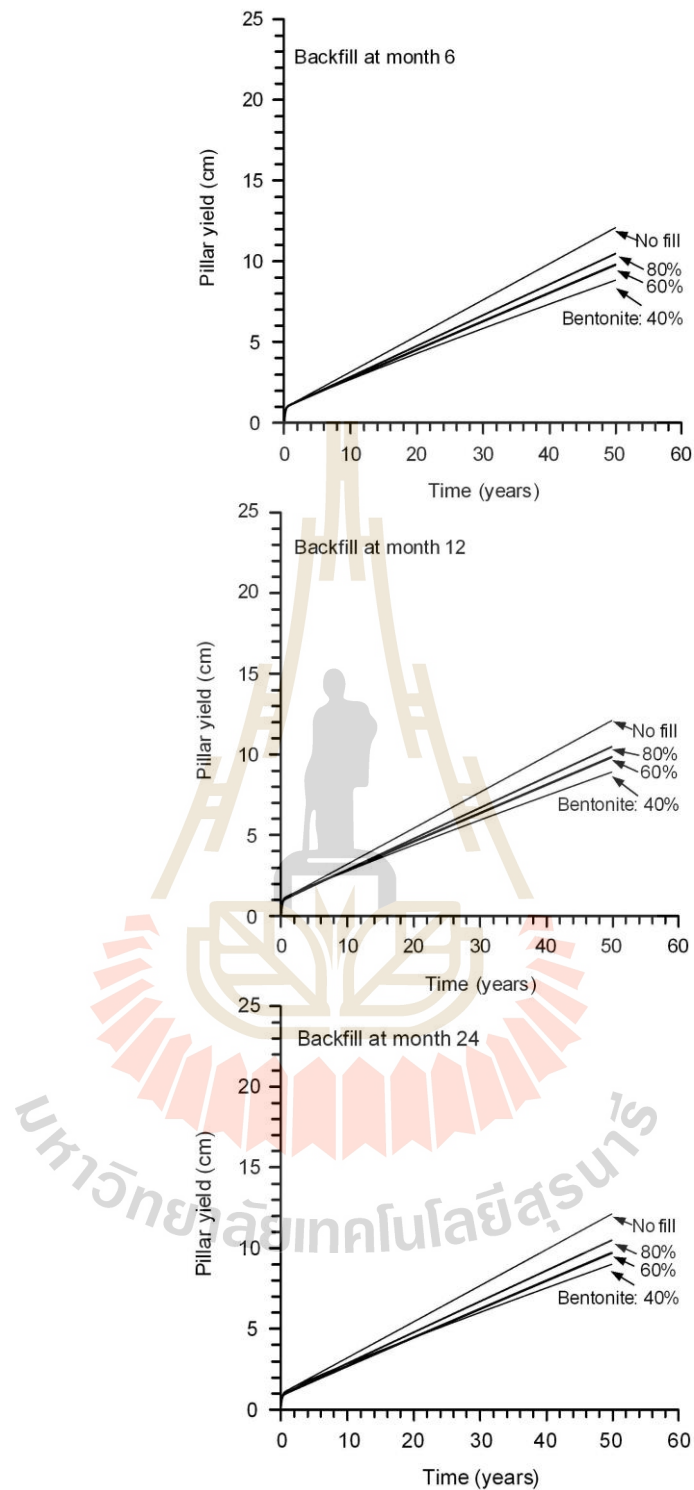


Figure 5.7 Pillar yield as a function of time with different B:C ratios where overburden thicknesses 200 m, duration before backfill 6, 12 and 24 months, and opening height 6 m.

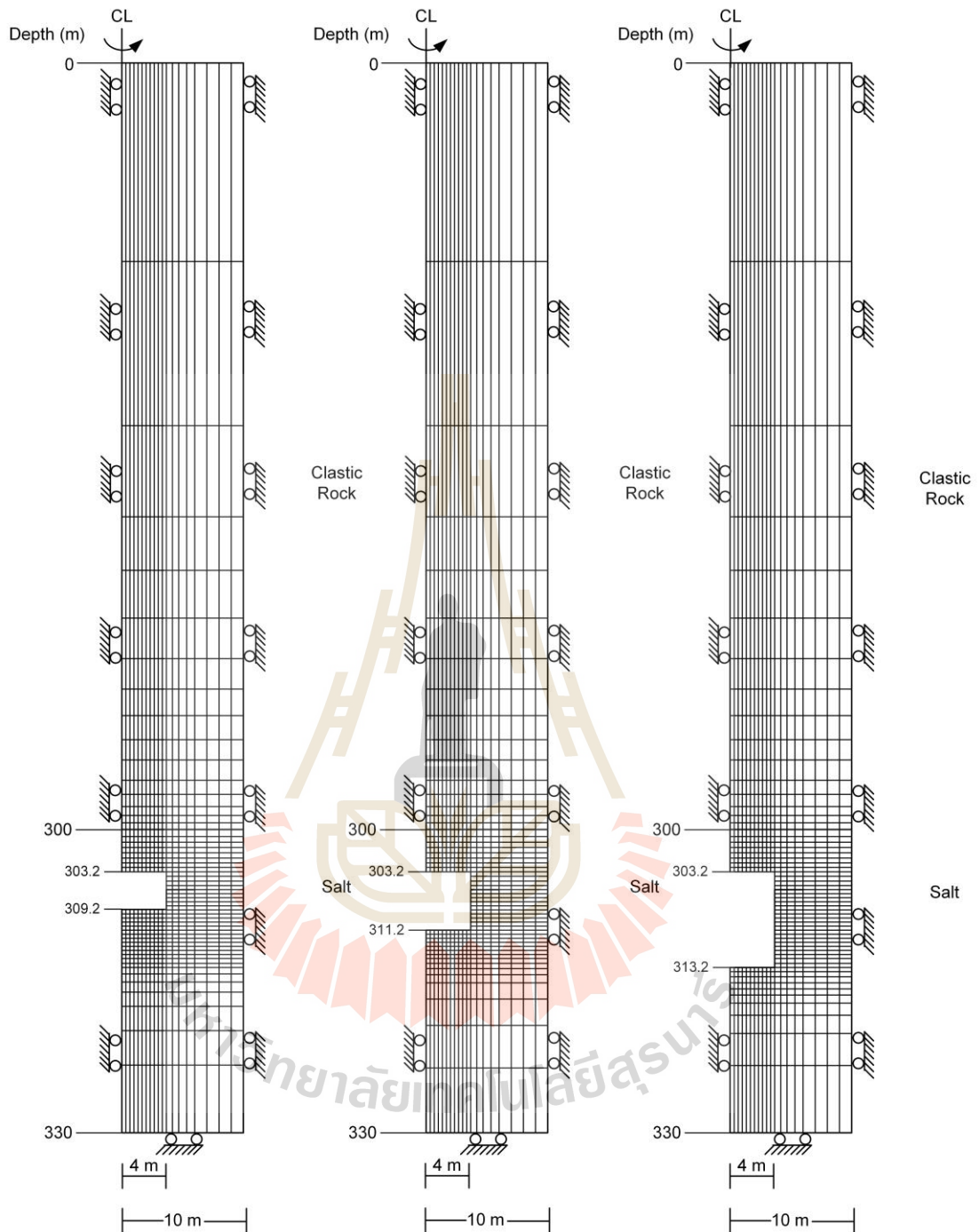


Figure 5.8 Finite difference mesh for opening height 6, 8 and 10 m, overburden thickness 300 m and rock salt 30 m.

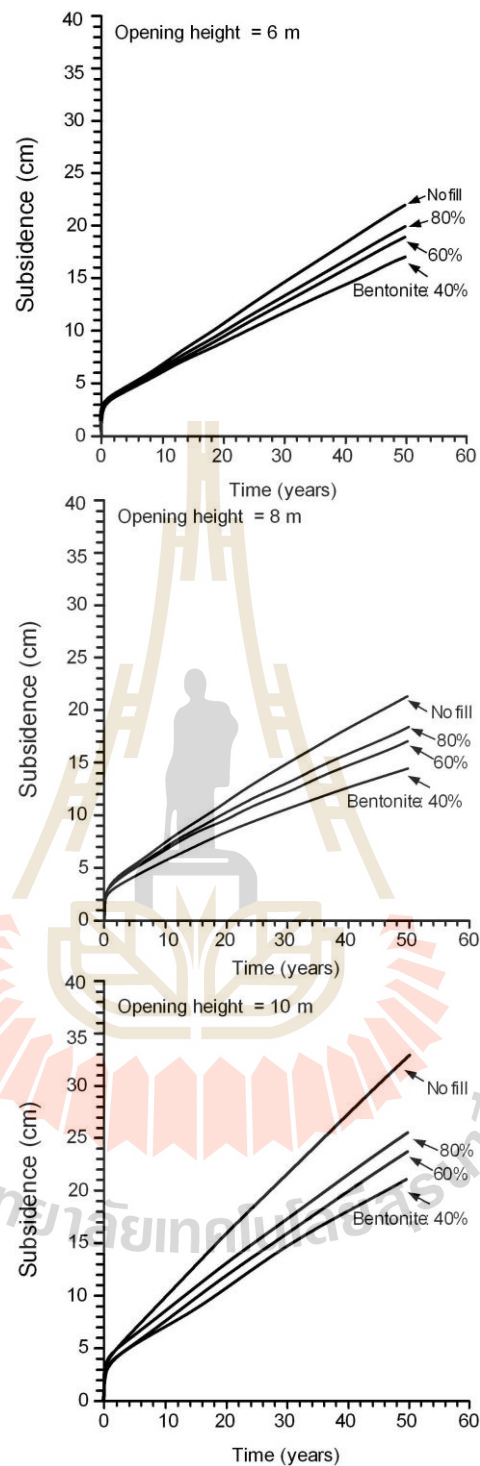


Figure 5.9 Surface subsidence as a function of time for different B:C ratios where opening height 6, 8 and 10 m, overburden thicknesses 300 m and duration before backfill 24 months.

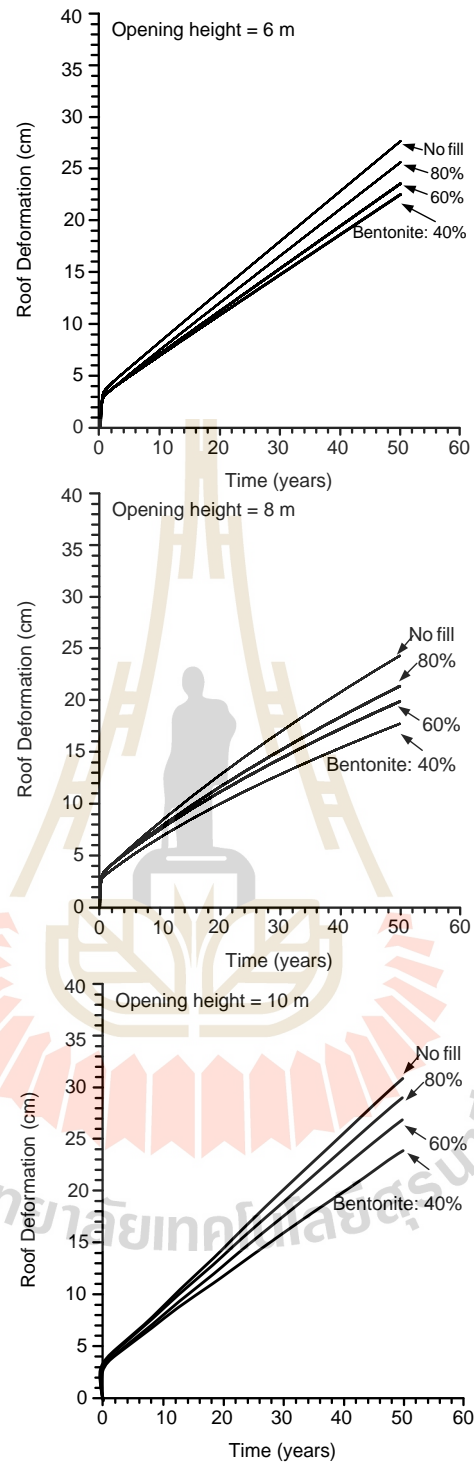


Figure 5.10 Roof deformation as a function of time for different B:C ratios where opening height 6, 8 and 10 m, overburden thicknesses 300 m and duration before backfill 24 months.

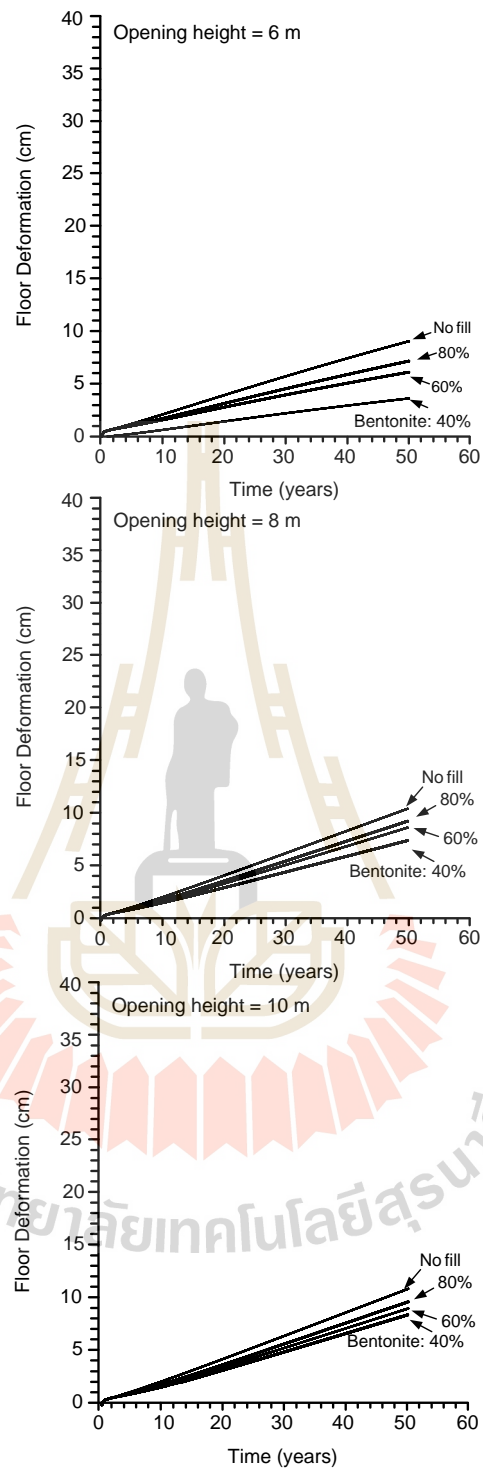


Figure 5.11 Floor heap as a function of time for different B:C ratios where opening height 6, 8 and 10 m, overburden thicknesses 300 m and duration before backfill 24 months.

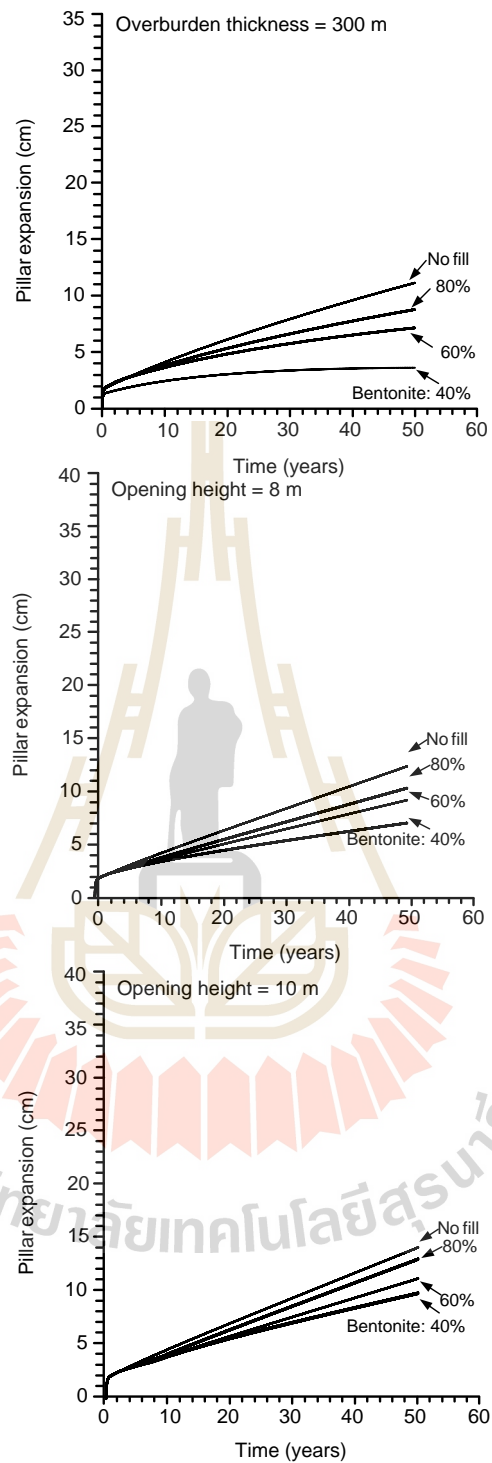


Figure 5.12 Pillar expansion as a function of time for different B:C ratios opening height 6, 8 and 10 m, overburden thicknesses 300 m and duration before backfill 24 months.

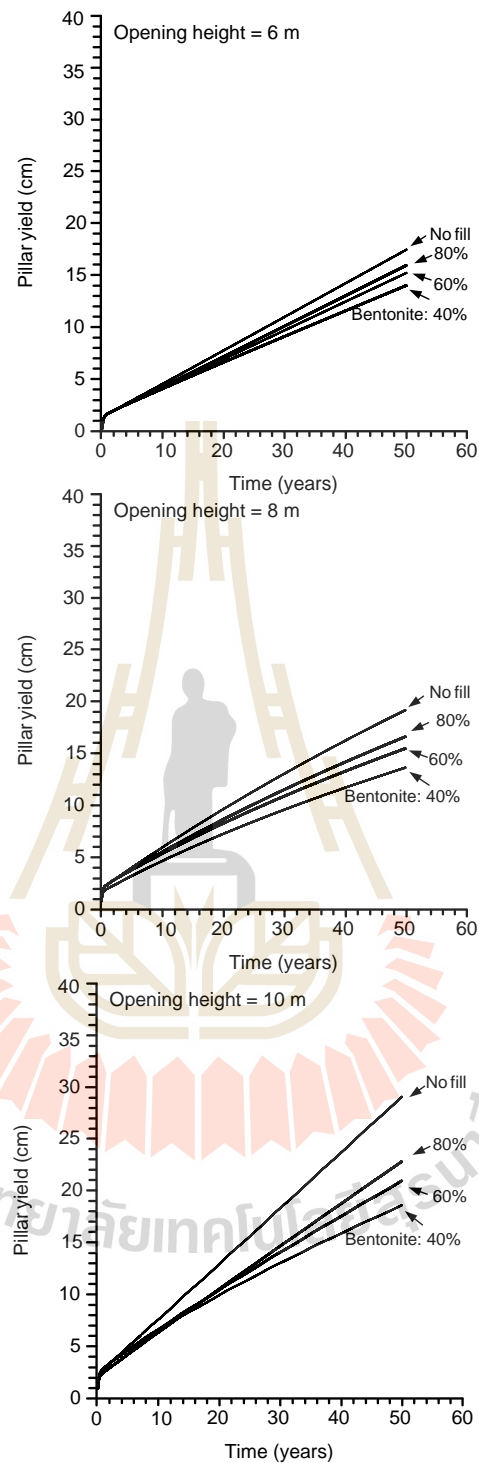


Figure 5.13 Pillar yield as a function of time for different B:C ratios where opening height 6, 8 and 10 m, overburden thicknesses 300 m and duration before backfill 24 months.

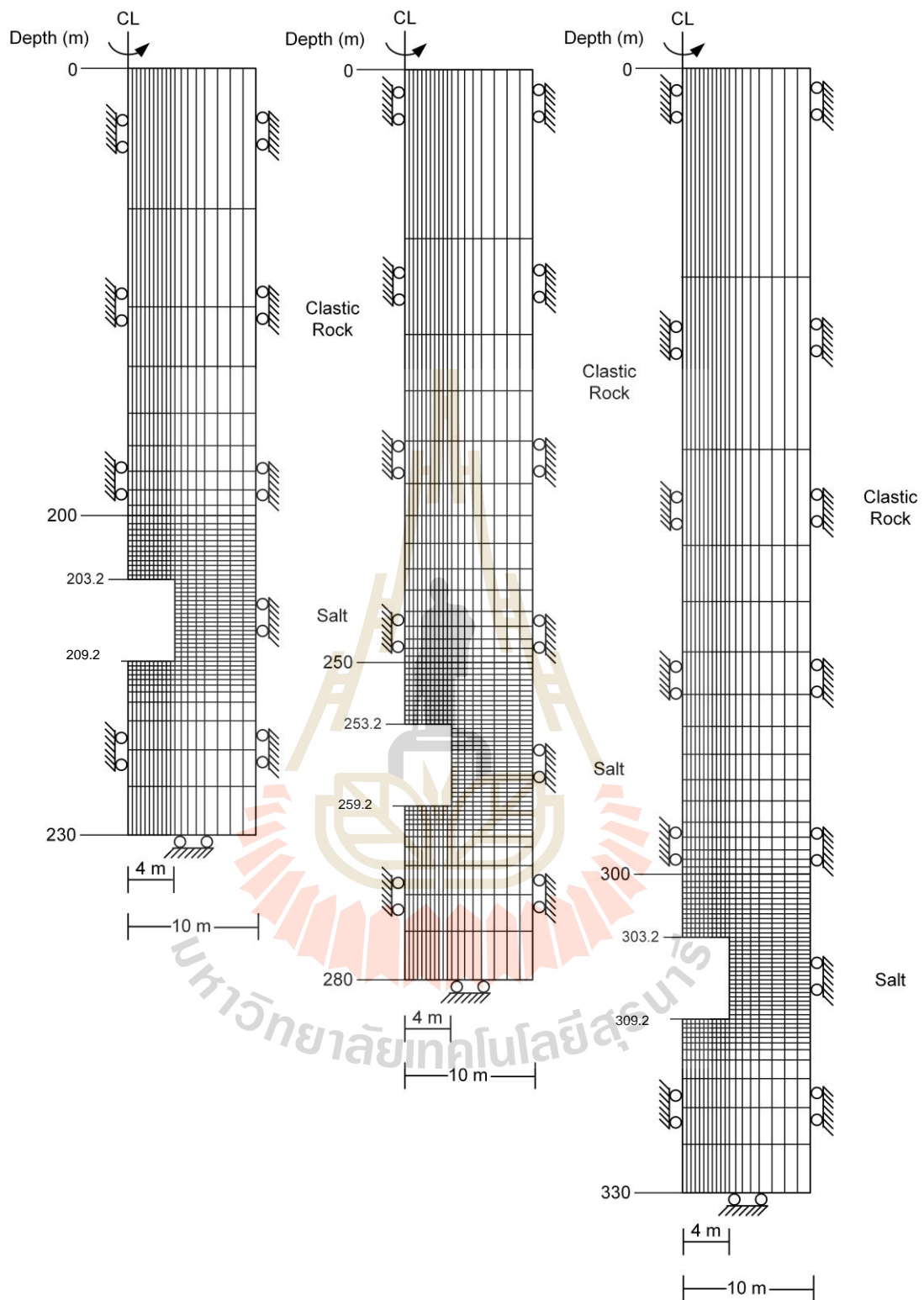


Figure 5.14 Finite difference mesh for overburden thickness 200, 250 and 300 m, rock salt 30 m and opening height 6 m.

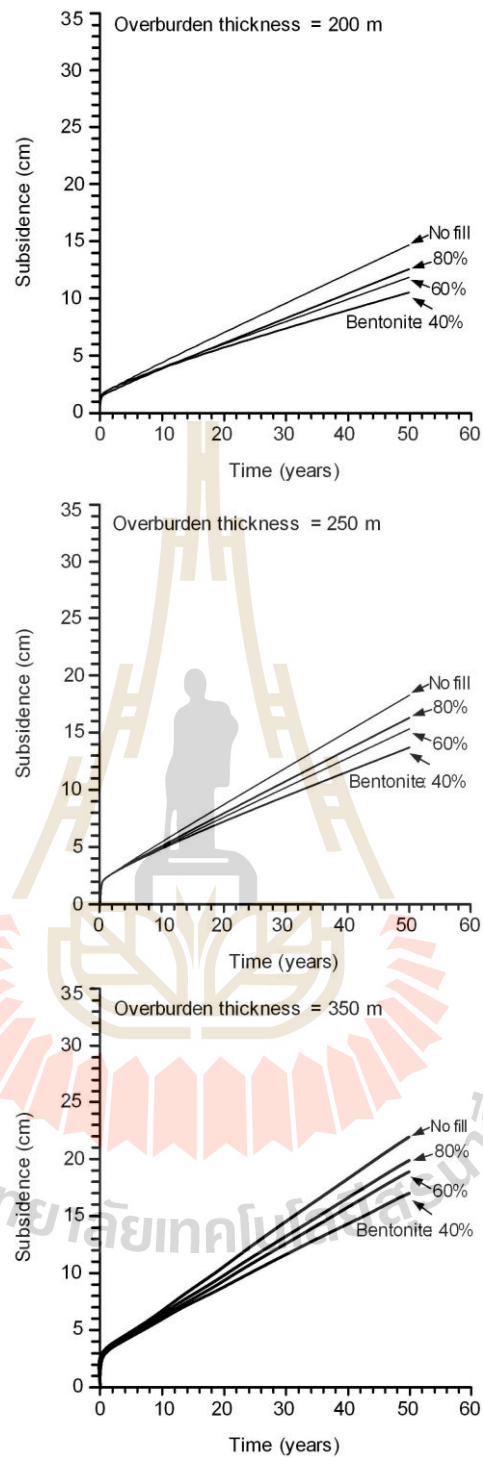


Figure 5.15 Surface subsidence as a function of time for different B:C ratios where overburden thicknesses 200, 250 and 300 m, duration before backfill 24 months and opening height 6 m.

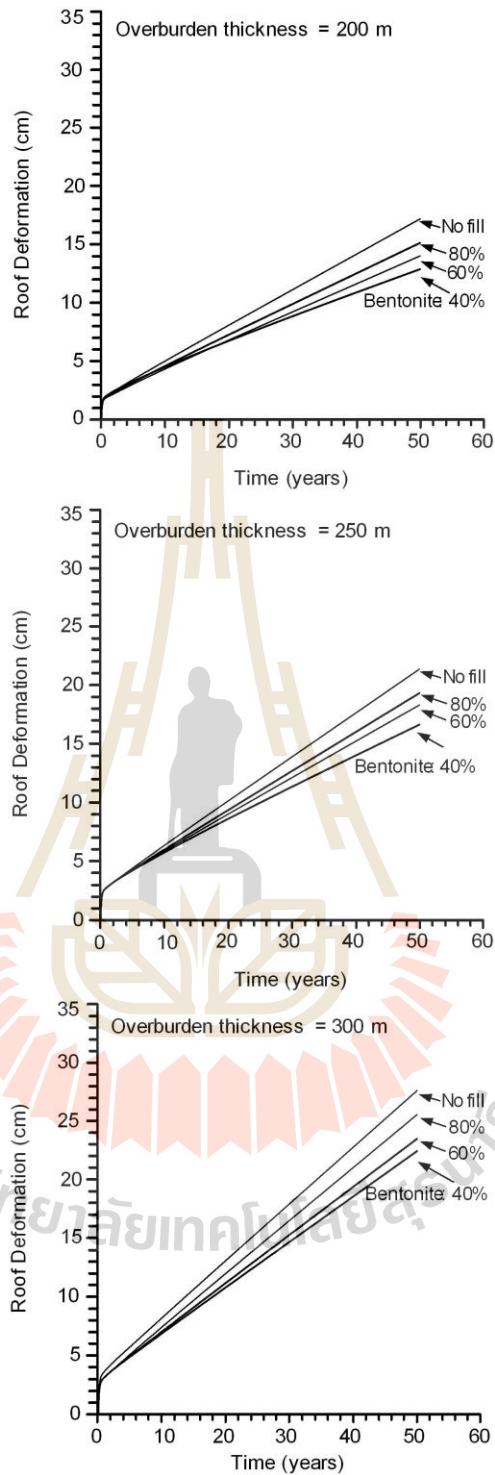


Figure 5.16 Roof deformation as a function of time for different B:C ratios where overburden thicknesses 200, 250 and 300 m, duration before backfill 24 months and opening height 6 m.

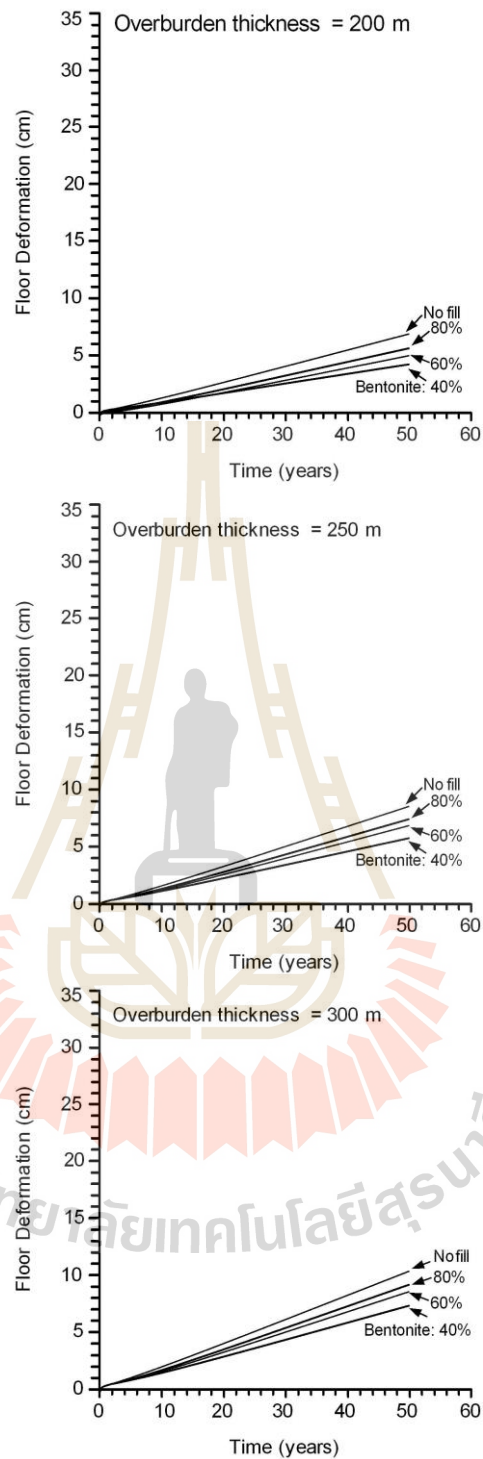


Figure 5.17 Floor heap as a function of time for different B:C ratios where overburden thicknesses 200, 250 and 300 m, duration before backfill 24 months and opening height 6 m.

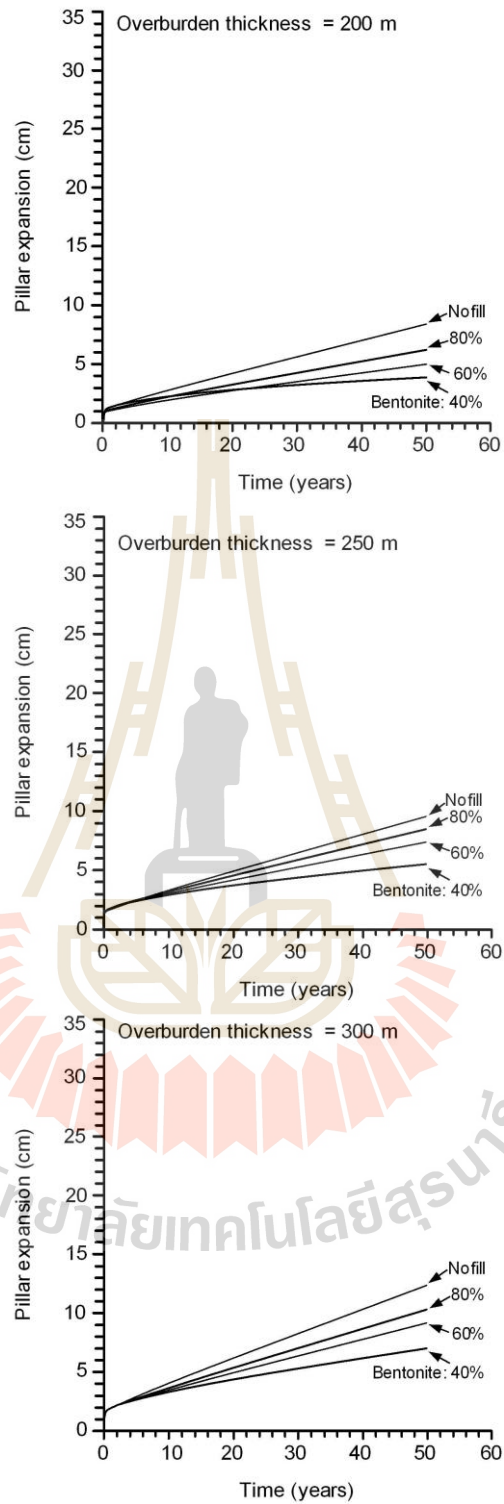


Figure 5.18 Pillar expansion as a function of time for different B:C ratios where overburden thicknesses 200, 250 and 300 m, duration before backfill 24 months and opening height 6 m.

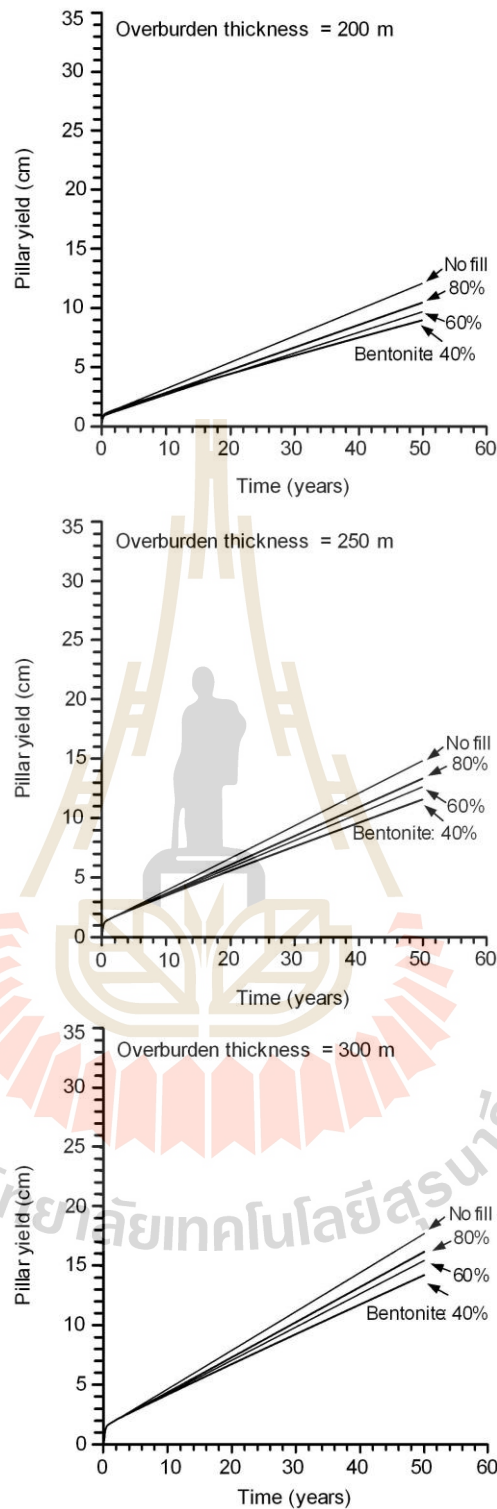


Figure 5.19 Pillar yield as a function of time for different B:C ratios where overburden thicknesses 200, 250 and 300 m, duration before backfill 24 months and opening height 6 m.

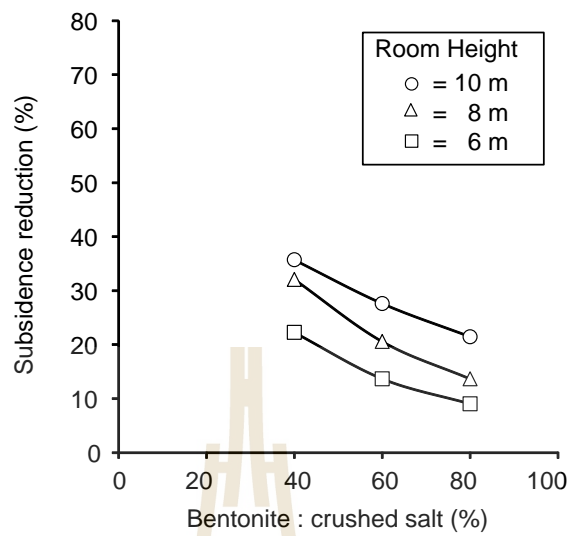


Figure 5.20 Subsidence reduction as a function of bentonite content.

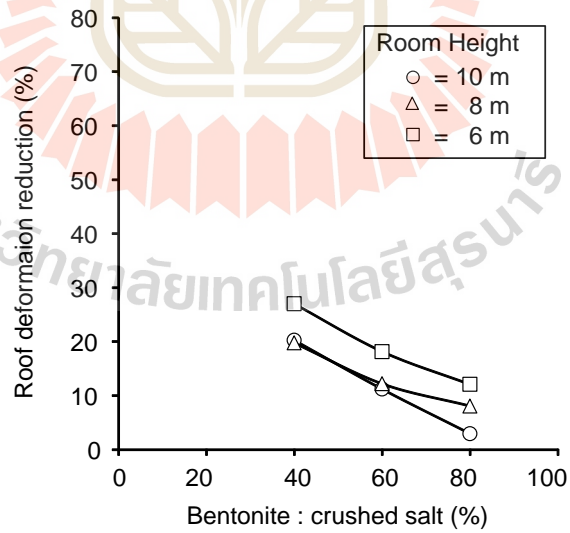


Figure 5.21 Roof deformation reduction as a function of bentonite content.

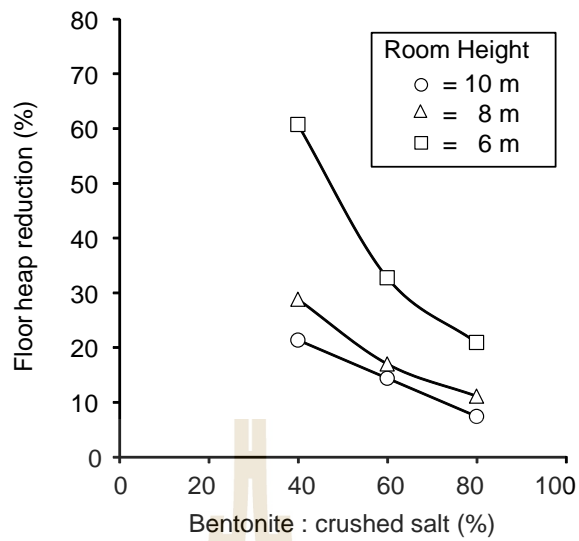


Figure 5.22 Floor heap reduction as a function of bentonite content.

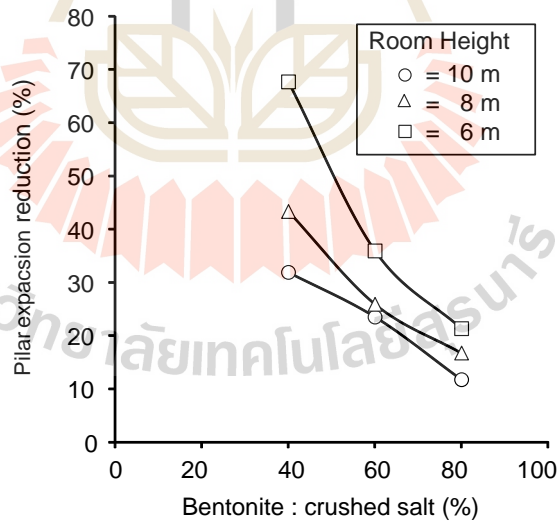


Figure 5.23 Pillar expansion reduction as a function of bentonite content.

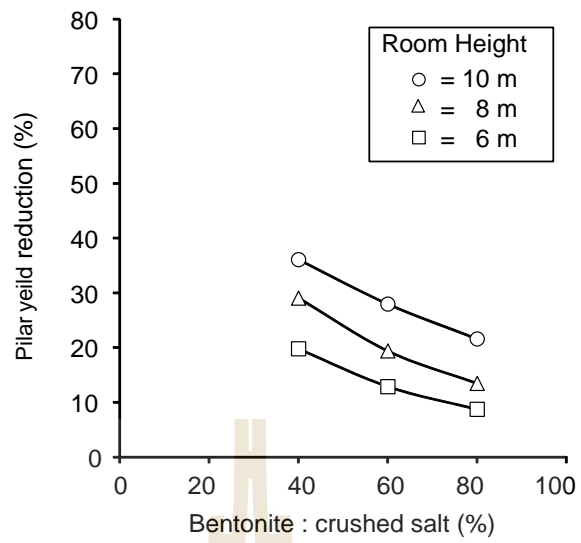


Figure 5.24 Pillar yield reduction as a function of bentonite content.



Table 5.4 Results of surface subsidence.

Condition parameter			Surface subsidence for 50 years (cm)			
Thickness overburden (m)	Duration before backfill (Months)	Opening height (m)	No fill	B:C = 80:20	B:C = 60:40	B:C = 40:60
200	6	6	14.69	12.71	11.76	10.37
200	12	6	14.69	12.57	11.79	10.42
200	24	6	14.69	12.57	11.47	10.54
250	24	6	18.28	16.31	15.33	13.71
300	24	6	21.98	19.99	18.98	17.09
300	24	8	21.40	18.48	17.00	14.53
300	24	10	32.79	25.75	23.74	21.09

Table 5.5 Results of roof deformation.

Condition parameter			Roof deformation for 50 years (cm)			
Thickness overburden (m)	Duration before backfill (Months)	Opening height (m)	No fill	B:C = 80:20	B:C = 60:40	B:C = 40:60
200	6	6	17.24	15.18	14.20	12.75
200	12	6	17.24	15.18	14.24	12.82
200	24	6	17.24	15.18	14.06	12.93
250	24	6	21.36	19.31	18.29	16.60
300	24	6	24.39	21.44	19.96	17.81
300	24	8	25.59	23.52	22.47	20.54
300	24	10	30.31	29.41	26.91	24.17

Table 5.6 Results of floor heap.

Condition parameter			Floor deformation for 50 years (cm)			
Thickness overburden (m)	Duration before backfill (Months)	Opening height (m)	No fill	B:C = 80:20	B:C = 60:40	B:C = 40:60
200	6	6	6.96	5.77	5.19	4.19
200	12	6	6.96	5.70	5.21	4.23
200	24	6	6.96	5.70	5.25	4.29
250	24	6	8.59	7.48	6.91	5.82
300	24	6	8.93	7.04	5.99	3.49
300	24	8	10.38	9.20	8.59	7.36
300	24	10	10.47	9.67	8.94	8.21

Table 5.7 Results of pillar expansion.

Condition parameter			Pillar expansion for 50 years (cm)			
Thickness overburden (m)	Duration before backfill (Months)	Opening height (m)	No fill	B:C = 80:20	B:C = 60:40	B:C = 40:60
200	6	6	8.38	6.33	5.27	3.67
200	12	6	8.38	6.20	5.31	3.74
200	24	6	8.38	6.20	5.38	3.86
250	24	6	9.45	8.38	7.28	5.41
300	24	6	11.82	9.31	7.59	3.84
300	24	8	12.42	10.36	9.22	7.06
300	24	10	14.33	12.67	10.98	9.78

Table 5.8 Results of pillar yield.

Condition parameter			Pillar yield for 50 years (cm)			
Thickness overburden (m)	Duration before backfill (Months)	Opening height (m)	No fill	B:C = 80:20	B:C = 60:40	B:C = 40:60
200	6	6	12.11	10.51	9.82	8.87
200	12	6	12.11	10.49	9.85	8.92
200	24	6	12.11	10.49	9.71	9.00
250	24	6	14.86	13.37	12.67	11.61
300	24	6	17.75	16.22	15.48	14.26
300	24	8	19.22	16.66	15.52	13.66
300	24	10	29.13	22.88	21.02	18.66

CHAPTER VI

DISCUSSIONS, CONCLUSIONS

RECOMMENDATIONS FOR FUTURE STUDIES

6.1 Discussions and Conclusions

- The results of compaction tests indicate that the increases of B:C ratios from 10:90 to 100:0 can decrease the maximum dry densities from 1.89 ton/m³ to 1.62 ton/m³, and increase the optimum brine contents from 2.8 % to 18.0 %. This agrees reasonably with the laboratory results obtained Cho et al. (1999), who perform the compaction tests on mixtures of bentonite and fine sand.
- As the B:C ratio increases, the friction angle and cohesion of the bentonite – crushed salt mixtures decrease. Similar test results are obtained by Sonsakul et al., (2013).
- Pure compacted bentonite can swell under saturated brine submersion up to 13% by volume within 30 days. Decreasing of the bentonite contents (or increasing the crushed salt contents) will decrease the swelling capacity of the mixtures. For B:C ratios of 40:60 the swelling capacity is reduced to about 4% by volume. This agrees with the experimental results obtained by Estabragh et al. (2013) and Wang et al. (2014). It should be noted that the swelling capacity may increase if more compactive effort (energy) is used to prepare the specimens. This behavior suggested by Kaufhold et al. (2015)

- The results from the swelling under loading show that the percentage of swelling by volume increases with decreasing the magnitude of the static loads on the mixtures. Similar observations are obtained by Kaufhold et al. (2015). The swelling capacity of high bentonite content mixtures is sensitive to the static loading magnitude more than that of the lower bentonite content ones. After the mixtures are oven-dried the swelling capacity of the mixtures for the next two wet-dry cycles tends to remain unchanged.

- The bentonite content can however decrease the strength and stiffness of the mixtures as shown in Table 4.3. The uniaxial compressive strength decreases from 0.79 MPa to 0.64 MPa for the mixtures with B:C ratios increases from 40:60 to 80:20. The deformation moduli also decrease from 0.84 GPa to 0.45 GPa.

- The results obtained from the computer modelling of subsidence reduction by bentonite-to-crushed salt backfill in mine openings indicate that the subsidence magnitudes increase with the mining depth and room height. The performance of backfill material tends to increase with increasing of room height. For example, the percentages of reduction of subsidence magnitude increase from 22.2, 32.1 to 35.7% for the mining depth of 300 m and room heights of 6, 8 and 10 m, respectively.

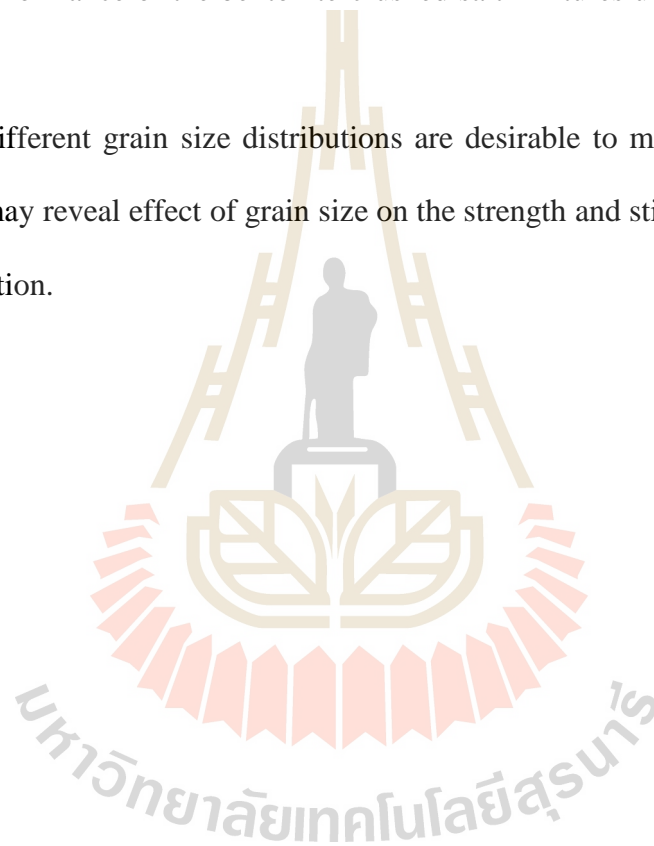
- Selections of suitable B:C ratios of the mixtures will depend on the site - specific needs. If swelling ability of the mixtures is important (such as the areas where minimization of groundwater circulation is required), high B:C ratio mixtures may be suitable more than the lower B:C ratio ones. On the contrary, in the areas where seal or backfill strength is more important than its swelling capacity, the lower B:C ratio mixtures may be more appropriate.

6.2 Recommendations for future studies

1. Different compactive effort (energy) should be used to obtain mixtures with different dry densities and brine contents. The results are useful for the design of the initial installation parameters of the bentonite-crushed salt backfill.

2. A greater number of wet-dry cycles should be performed to examine the long-term performance of the bentonite-crushed salt mixtures under saturated and dry cycles.

3. Different grain size distributions are desirable to mix with the bentonite. The results may reveal effect of grain size on the strength and stiffness of the mixtures after compaction.



REFERENCES

- Akgün, H., Ada, M. and Koçkar, M.K. (2015) **Performance assessment of a bentonite–sand mixture for nuclear waste isolation at the potential Akkuyu Nuclear Waste Disposal Site, southern Turkey.** Environmental Earth Sciences 73(10): 6101-6116.
- ASTM D1557-09. **Standard test method for laboratory compaction characteristics of soil using modified effort.** Annual book of ASTM standards, American Society for Testing and Materials, West Conshohocken, PA.
- ASTM D1883-16. **Standard Test Method for California Bearing Ratio of Laboratory-Compacted Soils.** Annual book of ASTM standards, American Society for Testing and Materials, West Conshohocken, PA.
- ASTM D2435-04. **Standard test method for one-dimensional consolidation properties of soil.** Annual book of ASTM standards, American Society for Testing and Materials, West Conshohocken, PA.
- ASTM D3080-04. **Standard test method for direct shear test of soil under consolidated drained condition.** Annual book of ASTM standards, American Society for Testing and Materials, West Conshohocken, PA.
- ASTM D422-07. **Standard test method for particle-size analysis of soil.** Annual book of ASTM standards, American Society for Testing and Materials, West Conshohocken, PA.

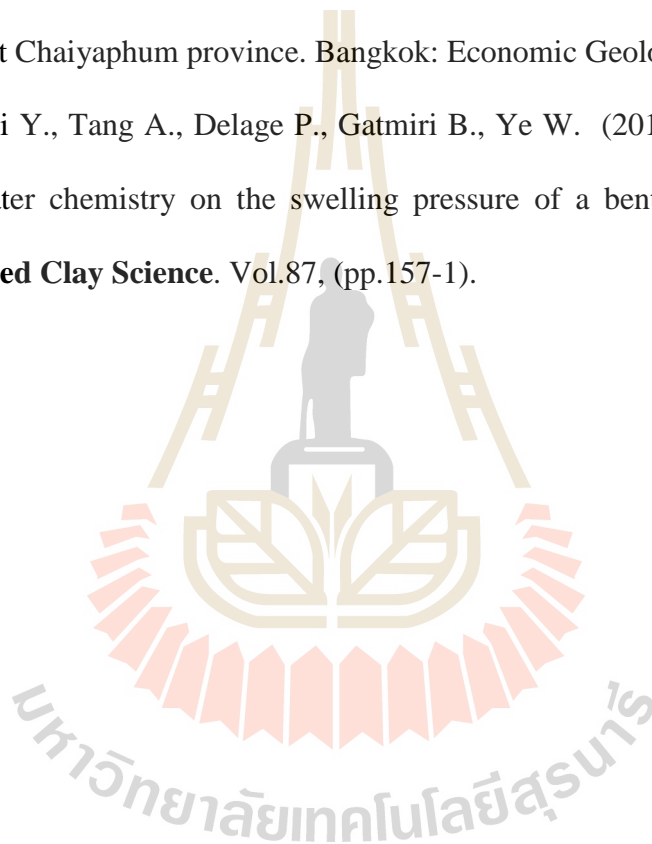
- ASTM D4318-05. **Standard test method for liquid limit, plastic limit, and plasticity index of soil.** Annual book of ASTM standards, American Society for Testing and Materials, West Conshohocken, PA.
- ASTM D5607-95. **Standard test method for performing laboratory direct shear strength test of rock specimens under constant normal force.** Annual book of ASTM standards, American Society for Testing and Materials, West Conshohocken, PA.
- ASTM D854-00. **Standard test method for specific gravity of soil solids by water pycnometer.** Annual book of ASTM standards, American Society for Testing and Materials, West Conshohocken, PA.
- ASTM Standard D698–07. **Standard Test Method for Laboratory Compaction Characteristics of Soil Using Standard Effort.** Annual book of ASTM standards, American Society for Testing and Materials, West Conshohocken, PA.
- Butcher, B.M. (1991). **The advantages of a salt/bentonite backfill for waste isolation pilot plant disposal rooms.** Technical Report No.SAND90-3074, Sandia National Laboratories, Albuquerque, NM.
- Case, J.B. and Kelsall, P. (1987). Laboratory investigation of crushed salt consolidation. **International Journal of Rock Mechanics and Mining Sciences and Geomechanics Abstracts.** 25(5): 216-223.
- Case, J.B., Kelsall, P.C. and Withiam, J.L. (1987). Laboratory investigation of crushed salt consolidation. In **Proceedings of the 28th U.S. Symposium on Rock Mechanics (USRMS).** Tucson, Arizona.

- Cho, W.J., Lee, J.O., and Kang, C.H. (2002). A compilation and evaluation of Mechanical properties of bentonite-based buffer materials for a high level waste repository. **Journal of the Korean Nuclear Society**. vol 34, (pp. 90-103).
- Crosby, K. (2007). Integration of rock mechanics and geology when designing the Udon South sylvinite mine. In **Proceedings of the First Thailand Symposium on Rock Mechanics** (pp. 3-22).
- Crosby, K.S. (2005). Overview of the geology and resources of the Udon Potash (sylvinite) deposits, Udon Thani province, Thailand. In **Proceedings of the International Conference on Geology, Geotechnology and Mineral Resources of Indochina** (pp. 283-299). Khon Kaen, Thailand.
- Daemen, J.J.K. and Ran, C. (1996). Bentonite as a Waste Isolation Pilot Plant Shaft Sealing Material. Contractor Report SAND96-1968. **Sandia National Laboratories**, Albuquerque, NM.
- Das, B. M. (2008). **Introduction to Geotechnical Engineering**. Ontario Canada: Thomson. pp.110-115.
- Das, B.M. (2010). **Principles of geotechnical engineering** (7th. Edn.), Cengage Learning, New York, pp. 666.
- Estabragh, A.R., Moghadas, M. and Javadi, A.A. (2013). Effect of different types of wetting fluids on the behaviour of expansive soil during wetting and drying. **Soil and Foundations**. Vol. 53(5), pp. 617-627.
- Fuenkajorn, K. (2007). Design process for sealing of boreholes in rock mass. In **Proceedings of the First Thailand Symposium on Rock Mechanics**, September, 13-14, Khao Yai, Thailand, Published by Geomechanics Research

- Unit, Suranaree University of Technology, Nakhon Ratchasima, Thailand, pp. 245-252.
- Fuenkajorn, K. and Daemen, J.J.K. (Eds.), 1996. **Sealing of Boreholes and Underground Excavations in Rock**. Chapman and Hall, London.
- Fuenkajorn, K., and Daemen, J.J.K. (1987). Mechanical interaction between rock and multi-component shaft or borehole plugs: Rock mechanics. **Rock Mechanics Proceedings of the 28th U.S. Symposium** (pp. 165-172). Rotterdam: A.A. Balkema.
- Hansen, F.D. (1997). Reconsolidating salt: compaction, constitutive modeling, and physical processes. **International Journal of Rock Mechanics and Mining Sciences**. 34(3-4): 119.e1–119.e12.
- Itasca (1992). **User Manual for FLAC-Fast Lagrangian Analysis of Continua**. Version 4.0, Minneapolis, Minnesota.
- Japakasetr, T. and Suwanich, P. (1977). Potash and rock salt in Thailand Bangkok: Economic Geology Division. **Department of Mineral Resources**. Bangkok.
- Japakasetr, T. (1985). Review on rock salt and potash exploration in Northeast Thailand. In **Proceedings Conference on Geology and Mineral Resources Development of the Northeast of Thailand** (pp. 135-147). Khon Kaen University, Thailand.
- Kaufhold, S., Baille, W., Schanz, T., and Dohrman, R. (2015). About differences of swelling pressure - dry density relations of compacted bentonites. **Applied Clay Science**. Vol.107, pp.52-61.

- Liu, C. (2011). Distribution laws of in-situ stress in deep underground coal mines. In **Proceedings conference on First International Symposium on Mine Safety Science and Engineering** (pp. 909-917). Beijing, China.
- Newman, N. and Zipf, R.K. (2005). Analysis of Highwall Mining Stability - The Effect of Multiple Seams and Prior Auger Mining on Design. In **Proceedings of the 24th International Conference on Ground Control in Mining** (pp. 208-217). Morgantown, West Virginia.
- Ouyang, S. and Daemen, J.J.K. (1989). **Crushed salt consolidation**. Rep. No. NUREG/CR-5402, Prepared by Department of Mining and Geological Engineering, University of Arizona.
- Pfeifle, T.W. (1991). **Consolidation, permeability, and strength of crushed salt/bentonite mixtures with application to the WIPP**. Rep. No. SAND90-7009, Sandia National Laboratories, Albuquerque, NM.
- Pusch, R. (1983). Borehole sealing for underground waste storage. **ASCE Journal of Geotechnical Engineering**. 109: 113–119.
- Ran, C., Daemen, J. J. K., Schuhen, M. D. and Hansen, F. D. (1997). Dynamic compaction properties of bentonite. **International Journal of Rock Mechanics and Mining Sciences**. 34(3-4): 253.e1-253.e19.
- Samsri, P., Sriapai, T., Walsri, C. and Fuenkajorn, K. (2010). Polyaxial creep testing of rock salt. In **Proceedings of the Third Thailand Symposium on Rock Mechanicson** (pp. 125-132). Thailand.
- Sonsakul, P., Walsri, C. and Fuenkajorn, K. (2013). Shear strength and permeability of compacted bentonite-crushed salt seals. In **Proceedings of the Fourth Thailand Symposium on Rock Mechanics** (99-109).Thailand.

- Sriapai. T., Chaowarin, W. and Fuenkajorn, K. (2012). Effects of temperature on compressive and tensile strengths of salt. **Science Asia**. 38: 166-174.
- Suwanich, P. and Ratanajaruraks, P. (1986). Sequences of rock salt and potash in Thailand (Nonmetallic Minerals Bulletin No. 1). Bangkok: Economic Geology, Division. **Department of Mineral Resources**. Bangkok.
- Suwanich, P., Ratanajaruraks, P. and Kunawat, P. (1982). Core log Bamnet Narong area at Chaiyaphum province. Bangkok: Economic Geology Division.
- Wang Q., Cui Y., Tang A., Delage P., Gatmiri B., Ye W. (2014). Long-term effect of water chemistry on the swelling pressure of a bentonite-based material. **Applied Clay Science**. Vol.87, (pp.157-1).



BIOGRAPHY

Miss Usachon Niewphueng was born on November 8, 1990 in Chaiyaphum Province, Thailand. She received her Bachelor's Degree in Engineering (Geotechnology) from Suranaree University of Technology in 2013. For her post-graduate, she continued to study with a Master's degree in the Geological Engineering Program, Institute of Engineering, Suranaree university of Technology. During graduation, 2014-2016, she was a part time worker in position of research associate at the Geomechanics Research Unit, Institute of Engineering, Suranaree University of Technology.

